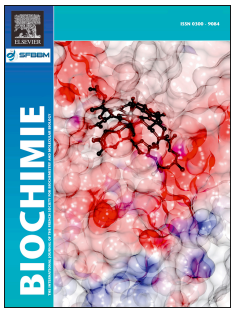

ConBr lectin modulates MAPKs and Akt pathways and triggers autophagic glioma cell death by a mechanism dependent upon caspase-8 activation

Ingrid A.V. Wolin, Isabella A. Heinrich, Ana Paula M. Nascimento, Priscilla G. Welter, Liliana del V. Sosa, Ana Lucia De Paul, Alfeu Zanotto-Filho, Cláudia Beatriz Nedel, Lara Dias Lima, Vinicius Jose Silva Osterne, Vanir Reis Pinto-Junior, Kyria S. Nascimento, Benildo S. Cavada, Rodrigo B. Leal

PII: S0300-9084(20)30279-0

DOI: https://doi.org/10.1016/j.biochi.2020.11.003

Reference: BIOCHI 6011

To appear in: *Biochimie*

Received Date: 15 July 2020

Revised Date: 26 October 2020

Accepted Date: 2 November 2020

Please cite this article as: I.A.V. Wolin, I.A. Heinrich, A.P.M. Nascimento, P.G. Welter, L.d.V. Sosa, A.L. De Paul, A. Zanotto-Filho, Clá.Beatriz. Nedel, L.D. Lima, V.J. Silva Osterne, V.R. Pinto-Junior, K.S. Nascimento, B.S. Cavada, R.B. Leal, ConBr lectin modulates MAPKs and Akt pathways and triggers autophagic glioma cell death by a mechanism dependent upon caspase-8 activation, *Biochimie* (2020), doi: https://doi.org/10.1016/j.biochi.2020.11.003.

ConBr lectin modulates MAPKs and Akt pathways and triggers autophagic glioma cell death by a mechanism dependent upon caspase-8 activation

Ingrid A.V. Wolin[1]; Isabella A. Heinrich[2]; Ana Paula M. Nascimento[1]; Priscilla G. Welter[1]; Liliana del V. Sosa[3,4]; Ana Lucia De Paul[3,4]; Alfeu Zanotto-Filho[5]; Cláudia Beatriz Nedel[6]; Lara Dias Lima[7]; Vinicius Jose Silva Osterne[7]; Vanir Reis Pinto-Junior[8]; Kyria S. Nascimento[7]; Benildo S. Cavada[7]; Rodrigo B. Leal[1,2]*

[1]Departamento de Bioquímica e Programa de Pós-graduação em Bioquímica, Centro de Ciências Biológicas, Universidade Federal de Santa Catarina, Campus Universitário, 88040-900 Florianópolis, Santa Catarina, Brazil

[2]Departamento de Bioquímica e Programa de Pós-graduação em Neurociências, Centro de Ciências Biológicas, Universidade Federal de Santa Catarina, Campus Universitário, 88040-900 Florianópolis, Santa Catarina, Brazil

[3]Centro de Microscopía Electrónica, Universidad Nacional de Córdoba, Facultad de Ciencias Médicas, Ciudad Universitaria, 5000 Córdoba, Argentina

[4]Consejo Nacional de Investigaciones Científicas y Técnicas (CONICET), Instituto de Investigaciones en Ciencias de la Salud (INICSA), Córdoba, Argentina

[5]Departamento de Farmacologia e Programa de Pós-graduação em Bioquímica, Centro de Ciências Biológicas, Universidade Federal de Santa Catarina, Campus Universitário, 88040-900 Florianópolis, Santa Catarina, Brazil

[6] Departamento de Biologia Celular, Embriologia e Genética, Laboratório de Biologia Celular de Gliomas, Programa de Pós-graduação em Biologia Celular e do Desenvolvimento, Universidade Federal de Santa Catarina, Campus Universitário, 88040-900 Florianópolis, Santa Catarina, Brazil

[7]Departamento de Bioquímica e Biologia Molecular, BioMolLab, Universidade Federal do Ceará, CEP 60020-181, Fortaleza, Ceará, Brazil

[8]Departamento de Física, Universidade Federal do Ceará, Fortaleza, Ceará, Brazil.

***Corresponding author**: Prof. Dr. Rodrigo Bainy Leal, Departamento de Bioquímica, Centro de Ciências Biológicas, Universidade Federal de Santa Catarina, Trindade, Florianópolis, Santa Catarina, Brazil, CEP 88.040-900; e-mail: rbleal@gmail.com; r.b.leal@ufsc.br

Abstract. Glioblastoma multiforme is the most aggressive type of glioma, with limited treatment and poor prognosis. Despite some advances over the last decade, validation of novel and selective antiglioma agents remains a challenge in clinical pharmacology. Prior studies have shown that leguminous lectins may exert various biological effects, including antitumor properties. Accordingly, this study aimed to evaluate the mechanisms underlying the antiglioma activity of ConBr, a lectin extracted from the *Canavalia brasiliensis* seeds. ConBr at lower concentrations inhibited C6 glioma cell migration while higher levels promoted cell death dependent upon carbohydrate recognition domain (CRD) structure. ConBr increased $p38^{MAPK}$ and JNK and decreased ERK1/2 and Akt phosphorylation. Moreover, ConBr inhibited mTORC1 phosphorylation associated with accumulation of autophagic markers, such as acidic vacuoles and LC3 cleavage. Inhibition of early steps of autophagy with 3-MA partially protected whereas the later autophagy inhibitor Chloroquine had no protective effect upon ConBr cytotoxicity. ConBr also augmented caspase-3 activation without affecting mitochondrial function. Noteworthy, the caspase-8 inhibitor IETF-fmk attenuated ConBr induced autophagy and C6 glioma cell death. Finally, ConBr did not show cytotoxicity against primary astrocytes, suggesting a selective antiglioma activity. In summary, our results indicate that ConBr requires functional CRD lectin domain to exert antiglioma activity, and its cytotoxicity is associated with MAPKs and Akt pathways modulation and autophagy- and caspase-8- dependent cell death.

KEYWORDS: Lectin; ConBr; Glioma; Autophagy; Akt/mTORC1; Cell signaling

1. Introduction

Glioblastoma multiforme (GBM) is considered the most aggressive primary malignant brain tumor of the central nervous system (CNS) in adults, with a median survival of 14.2 months despite some advances in therapy over the last decades [1,2]. Numerous genetic alterations, such as gene mutations, deletions and amplifications, as well as intratumoral heterogeneity, are associated with the fast-proliferation and highly invasive phenotypes that lead to rapid tumor progression and poor prognosis in high-grade gliomas [1]. The cellular phenotypes observed in GBM demonstrate a connection between mutated gene and modification of key cell survival pathways, including PI3K/PTEN-Akt-mTORC1 and MAPK pathways, to cite a few [2,3]. It has been suggested that overexpression of *N*-acetylgalactosaminyltrasferase 2 (GALNT2), an enzyme that regulates the initial step of mucin *O*–glycosylation, facilitates the malignant characteristic of glioma by influencing the *O*-glycosylation and phosphorylation of EGFR and the subsequent downstream PI3K/Akt/mTOR pathway *in vitro* and *in vivo* [4]. Moreover, it has been demonstrated that drug-resistant cancer cells typically express distinctive glycosylated antigens [5]. Overall, it is well established that glycan alteration may lead impairment of cell-cell adhesion, activation of oncogenic signaling pathways, deregulation in proliferation and cell death mechanisms, induction of pro-metastatic phenotypes and trigger adaptive chemoresistance [6,7]. Regarding the importance of glycosylation in pathophysiology of cancer, the use of molecules capable of recognizing these differentiated structures has only drawn more attention in the last years, with the availability of a crescent number of studies characterizing the structure of animal and plant lectins. These facts call for the development of novel antiglioma compounds capable of inhibiting survival responses using glycosylated molecules as molecular targets [2,5].

Lectins are a ubiquitously distributed group of proteins of nonimmune origin that containing at least one non catalytic domain (carbohydrate recognition domain; CRD) that selectively recognizes and reversibly binds to specific free sugars, as well as carbohydrate structures present on glycoproteins and glycolipids [8–10]. Lectins extracted from plants comprise a group of homologous proteins that assumed to play an important role in plant resistance and development, and which have captured pharmacological and biological interest. For example, with their ability to recognize glycosylation patterns present on the cancer cell surface, along with cytotoxic activity,

lectins have been suggested as a potential tool for recognition of cancer cells and selective treatment [11–16].

Legume seeds are a rich source of lectins, and several genres of the *Diocleinae* subtribe showed an important source for isolation and characterization of these proteins [17–20]. ConA, a lectin isolated one hundred years ago from *Canavalia ensiformis* seeds, displays mannose/glucose-binding specificity [21,22], and it is the foremost studied lectin of this subtribe, exhibiting diverse biological actions, including antitumor activity via induction of apoptosis [22,23] or autophagy [15,24–26]. After isolation and characterization of ConA, other lectins from the same subtribe were purified and characterized for their biological effects. Of note, we previously demonstrated that ConV (*Canavalia virosa* lectin), CaBo (*Canavalia bonariensis* lectin), DLL (*Dioclea lasiocarpa* lectin) and DlyL (*Dioclea lasiophylla* lectin) all present cytotoxic effects on C6 glioma cells [12,27–29], although the cell death mechanisms remains poorly understood. Moreover, the glucose/mannose-specific lectin isolated from the seeds of the legume plant *Dioclea violacea* (DVL) showed more prominent antiglioma activity than ConA against C6 [27] and U87 glioma cell lines [30].

ConBr, a lectin purified 40 years ago from *Canavalia brasiliensis* seeds, is also known as Cow Bean, a native legume (subtribe *Diocleinae*) of Brazil and South America. It is a glucose/mannose-specific lectin largely homologous to ConA, differing by only three residues [31,32]. Numerous studies have shown various biological actions of ConBr on different targets, including immune and nervous system cells [33–35]. Besides, ConBr exerted antiproliferative effects on leukemia [36] and melanoma cell lines [37], even though the mechanisms involved in ConBr anticancer effects remain unknown. Prior studies from our group have also demonstrated antidepressant-like effects of ConBr on animal models, which seems to involve induction of Brain-derived neurotrophic factor (BDNF) expression *in vivo*, as well as neuroprotective responses of ConBr *in vivo* and *in vitro* [38–43]. Therefore, considering the antitumor potential of legume lectins and the biological effects of ConBr in different models, the present study was carried out to investigate the antiglioma activity of ConBr and the molecular mechanism underlying this process.

2. Materials and Methods

2.1 Materials

High-glucose Dulbecco's Modified Eagle's Medium (DMEM), trypsin, and fetal bovine serum (FBS) were purchased from Gibco®. Penicillin, streptomycin, 3-(4,5-dimethylthiazol-2-yl)-2,5-diphenyltetrazolium bromide (MTT), Hoechst, Propidium iodide (PI), Acridine Orange (AO), Cloroquine (CQ), 3-methyl-adenine (3-MA) and Temozolomide (TMZ) were from Sigma®; FLICE Inibitor (1mM IETD-fmk) was obtained from Clontech and Annexin-V-FITC from Life Technology®. The following antibodies were acquired as follows: Atg7 (#8558 - Cell Signaling®), LC3A/B (#12741 - Cell Signaling®), Beclin-1 (#3495- Cell Signaling®), pmTORC1(#2971 – Cell Signaling®), mTORC1 (#2972 – Cell Signaling®), pJNK (#92515 - Cell Signaling®), JNK (#559304 - Sigma®); pAkt (#92715 - Cell Signaling®), Akt (#46855 - Cell Signaling®), pERK1/2 (#M8159 - Sigma®), ERK1/2 (#M5670 - Sigma®), p-$p38^{MAPK}$ (#9211- Millipore®), and $p38^{MAPK}$ (#9211- Sigma®), Bak (#12105 – Cell Siganaling®), BNIP3 (#3769 – Cell Signaling®), Puma (#12450– Cell Signaling®), Bad (#9239 – Cell Signaling®), pBad ((Ser112) #5284– Cell Signaling®) and β-actina (#47778 – Santa Cruz®). Rat C6 glioma cells (ATCC-CCL-107) and human U87 glioma cells (ATCC/HTB-14) were provided by the Cell Bank of Rio de Janeiro (RJ, Brazil). Isolation and culturing of primary cortical astrocytes and Glioblastoma Multiforme (GBM1) cultures were performed at Universidade Federal de Santa Catarina (UFSC) as described below. All procedures were approved by appropriated local Ethical Committees.

2.2 ConBr purification

ConBr was purified from powdered *Canavalia brasiliensis* seeds as described previously [44]. In short, seeds were collected in Ceará State, and ground in a coffee grinder (Cadence™ MDR301 Monovolt, Cadence Design Systems, San Jose, CA, USA) to obtain a fine powder. Soluble proteins were extracted in 150 mmol L^{-1} NaCl (1:10 w/v) under continuous stirring by 4 h at 25 °C, followed by centrifugation at 10,000 x *g* at 4 °C for 20 min. The supernatant was applied to a Sephadex G-50 column (5 x 25 cm) previously equilibrated with 150 mmol L^{-1} NaCl containing 5 mmol L^{-1} $CaCl_2$ and 5 mmol L^{-1} $MnCl_2$. Unbound proteins were eluted with the same equilibration solution. The bound lectin was eluted with 0.1 M glycine (pH 2.6) containing 150 mmol L^{-1} NaCl, subsequently dialyzed against distilled water, and then lyophilized. The purity of samples was confirmed by SDS-PAGE (15 % gel).

2.3 Glioma cell cultures

The rat C6 glioma cell line and human U87 glioma cell line were maintained in Dulbecco's Modified Eagle's Medium (DMEM) supplemented with 10% (v/v) fetal bovine serum (FBS) (Gibco®), 100 units/mL penicillin and 100 mg/mL streptomycin (Gibco®), at 37 °C in a humidified atmosphere of 95% air and 5% CO_2 [27, 30]. GBM-1 cells were isolated from a GBM tumor surgically taken from a 64 years-old female patient at Hospital Celso Ramos Hospital in Florianopolis, Santa Catarina [45]. The tumor was collected in 15 mL DMEM: Nutrient Mixture F-12 (DMEM-F12) containing 10% FBS, cerebral meninges and blood vessels were removed, and the tissue was mechanically dissociated with trypsin and the aid of a Pasteur pipette. Then the cells were washed with phosphate buffer saline (PBS) (140 mM NaCl, 3 mM KCl, 10 mM Na_2HPO_4 and 2 mM KH_2PO_4, pH 7.4) and cultured in petri dish containing DMEM-F12 plus glucose (0.6%), glutamine (2 mM), sodium bicarbonate (0.06%) and penicillin/streptomycin (100 units/ 100 µg for mL) and supplemented with 10% FBS. The cells were kept at 37 °C in a humidified atmosphere of 95% air and 5% CO_2. All procedures and patient consent forms were approved by the UFSC Human Research Ethics Committee (CEPSH protocol number 108.286).

2.4 Treatments

For an initial screening, after reaching cell confluence, C6, U87MG and GBM1 cells were treated with ConBr 1, 10, 30 and 50 µg/mL (10, 100, 300 and 500 nM, respectively) or vehicle for 24 h (Supplementary Figure X1) and cell morphology and viability (MTT assay) were assessed. C6 glioma cells were chosen to continue the experiments. Hence, they were seeded in 96-, 48- or 6-well plates, respectively, and incubated for 24 h at 37 °C in an incubator at 80% confluence, the culture medium was changed, and the cells were incubated in complete DMEM containing either vehicle or ConBr lectin 1, 10, 30 or 50 µg/mL concentrations for different time points depending on the experiment. C6 glioma cells treated with multiple concentrations of TMZ (100, 200, 300, 400 and 500 µM) for 24 h were used as a positive control in order to compare the magnitude effect of ConBr with a clinically approved antiglioma agent (Supplementary Figure X4). ConBr was dissolved with HEPES–saline buffer without glucose composed of NaCl 124 mM, KCl 4 mM, $MgSO_4$ 1.2 mM, HEPES 25 mM, and $CaCl_2$ 1 mM, pH 7.4. Throughout the experiments, "control" group consisted of ConBr

vehicle (HEPES–saline buffer without glucose). To evaluate whether the action of ConBr was dependent on its carbohydrate-recognition domain, ConBr was blocked by diluting the lectin in glucose-free HEPES-saline buffer containing 0.1 M of its specific binding sugar (α-methyl-D-mannoside) and maintained for 30 minutes at 37 °C before treating cells. Aiming to evaluated the role of autophagy and caspase-8 in C6 glioma cell viability, we performed experiments with 3-methyl-adenine (3-MA), Chloroquine (CQ, Sigma®) and FLICE inhibitor (1mM IETD-fmk) from Clontech® [46,47]. 3-MA inhibits autophagy by blocking autophagosome formation via the inhibition of class III PI3K [48] and CQ is a fusion blocker between autophagosome and lysosome [49,50]. 3-MA and CQ were used at 2 mM and 10 µM concentrations, respectively, added to the cells at 1 h prior to ConBr treatment. IETD-fmk was used at 2 µM pretreatment for 6 h prior to ConBr incubation.

2.5 Light microscopy

Morphological alterations of glioma cells in response to lectin treatment were evaluated in cells seeded in 96-well plates at 10^4 cells/well, and incubated for 3, 6, 12, 24 or 48 h with ConBr. At the end of treatments, the cells were observed by light microscopy by using an inverted NIKON eclipse T2000-U microscope.

2.6 MTT assay

Cell viability was estimated by MTT (Sigma®) [30-(4,5-dimethylthiazol-2yl) 2,5-diphenyltetrazolium bromide] reduction assay as previously described [51]. Briefly, glioma cells were seeded in 96-well plates at 10^4 cells/well and incubated for 24 h with vehicle or ConBr. In addition, the C6 cells were treated by 3, 6, 12, 24 or 48 h with the same treatment to perform a time/concentration response curve. After treatment, the medium was removed, and cells were incubated for 1 h at 37 ^{o}C with 100 µL of 0.5 mg/mL MTT dissolved in HBSS. Reduced MTT formazan crystals were dissolved with 100 µL dimethylsulfoxide (DMSO) for 30 min at 37 ^{o}C, and the absorbance evaluated at 540 nm using a Tecan® Microplate Reader Infinite M200 reader, equipment at the Laboratório Multiusuário de Estudos em Biologia at the Universidade Federal de Santa Catarina (LAMEB/UFSC). The results were expressed as a percentage of the control/vehicle group (considered as 100% viable).

2.7 Lactate Dehydrogenase (LDH) assay

The leakage of LDH into the cell culture medium was measured as an estimate of cell membrane integrity, as described by Rosa et al. [52]. To this end, C6 glioma cells were seeded in a 96-well plate at 10^4 cells/well and incubated for 12 or 24 h with vehicle or ConBr. At the end of treatments, 50 µL of cell culture medium was mixed with 200 µL of 0.5 M potassium phosphate buffer containing pyruvate, NaHCO3 and NADH, and the kinetics of LDH enzymatic activity was monitored at 340 nm using an Infinite M200 (Tecan®) reader. Cells incubated with 0.02% Triton-X100 (added 15 min prior to medium harvesting) were used as a positive control for LDH activity. Delta NADH absorbance was converted to percentages relative to positive controls (Triton-X100 treated cells; considered as 100% LDH leakage).

2.8 JC-1 assay

The mitochondrial membrane potential (ΔΨm) was measured using the 5,5′,6,6′-tetrachloro-1,1′,3,3′-tetraethyl-benzimidazolyl carbocyanine iodide (JC-1) (modifications of De Biasi et al. [53]). C6 cells were seeded in 96-well plates at 10^4 cells/well for 24 h and then treated for 6 h with vehicle/control or ConBr. Carbonyl cyanide 4-(trifluoromethoxy) phenylhydrazone (FCCP, 1 µM; Sigma®) treated cells were also carried out as a positive control for mitochondrial depolarization. At the end of treatments, de medium was replaced with 0.1 mL of 1 mM JC-1 solution, and the cells incubated for 20 min at 37 °C protected from light. Thereafter, the cells were washed with PBS (140 mM NaCl, 3 mM KCl, 10 mM Na2HPO4 and 2 mM KH2PO4, pH 7.4), followed by the addition of 0.1 mL/well PBS. Fluorescence was measured in a Spectramax Paradigm Microplate Reader (Molecular Devices®, Sunnyvale, CA, USA) set at 490 nm excitation and 520 nm emission for detection of red fluorescence (J-aggregates) and 525 nm excitation and 590 nm emission for green detection (JC-1 monomers). The values of red/green fluorescence ratio of each sample were converted to percentages relative control/vehicle-treated cells. The assays were performed in 4 independent experiments in triplicate.

2.9 ROS assay

Reactive oxygen species (ROS) production was evaluated by using the 2,7-dichlorodihydrofluorescein diacetate (H2DCF-DA) fluorescent probe [29]. Briefly, C6 cells were plated in a 96-well plate at 10^4 cells/well for 24 h and then treated with ConBr or vehicle for 6 h. The culture medium was removed, the cells were washed with

PBS, and then 100 µL of 10 µM H2DCF-DA was incubated at 37 °C for 20 minutes. The H2DCF-DA solution was discarded, the cells were washed with PBS, and 100 µL PBS was added for fluorescence reading at 485/520 nm (excitation/emission) using a SpectraMax® reader (Molecular Devices), equipment at the Laboratório Multiusuário de Estudos em Biologia at the Universidade Federal de Santa Catarina (LAMEB/UFSC). Cells treated with 100 µM hydrogen peroxide (H_2O_2) for 15 minutes were used as a positive control for ROS production.

2.10 Acridine Orange staining of acidic vesicular organelle

Acridine Orange (AO) assay was performed to evaluate acidic vesicular organelle (AVO) formation by ConBr. C6 cells were seeded in a 96-well plate at 10^4 cells/well for 24 h in complete DMEM. Then, C6 cells were treated with vehicle (control) or ConBr for 3, 6, 12, 24 or 48 h, after treatment period, 50 µL of culture medium was removed and was added 20 µL of AO (10 µg/mL; Sigma®) for 20 min in the dark at 37 ºC (modifications of Singh et al. [54]). The cells were visualized by an inverted NIKON eclipse T2000-U microscope using filter sets of 470 nm excitation and 525 nm emission for chromatin (CR; green fluorescence) and 350 nm excitation and 615 nm emission for acidic vesicular organelles (AVO; orange/red fluorescence) detection.

2.11 Propidium Iodide staining

For Propidium Iodide (PI) assay, C6 cells were seeded in a 96-well plate and treated in the same conditions as described for the Acridine Orange assay. At the end of treatments, the cells were incubated with Hoechst (1 mg/mL - Sigma®) and PI (1 mg/mL - Sigma®) at final concentration of 0.015 mg/mL for 15 min in the dark (modifications of Singh et al. [54]). The cells were visualized in an inverted NIKON eclipse T2000-U microscope using filter sets of 488 nm excitation and 560 nm emission for PI and 353 nm excitation and 483 nm emission for Hoechst.

2.12 Transmission electron microscopy (TEM)

TEM analysis was performed as previously described by De Paul et al. [55]. C6 cells (6 x10^6 cells) were seeded in 25 cm^2 flasks and cultured for 24 h. Afterwards the medium was replaced with a new medium containing vehicle or ConBr at 30 µg/mL for 12 h. At the end of treatments, the cells were trypsinized, and cell pellets fixed in

Karnovsky mixture containing 4% formaldehyde and 2% glutaraldehyde in 0.1 M cacodylate buffer plus 7% sucrose. Then, the cells were treated with 1% OsO4 for 1 h, followed by staining-in-block with 1% uranyl acetate in 0.1 M acetate buffer pH 5.2 for 20 min. After dehydration with a series of graded cold acetone, the cells were embedded in Araldite resin (Electron Microscopy Sciences, Hatfield, PA). Thin sections were cut using a JEOL ultramicrotome (Nikon, Tokyo, Japan) with a diamond knife and then stained with uranyl acetate/lead citrate and examined using a Zeiss Leo 906-E electron microscope equipped with the digital camera Megaview III (Oberkochen, Germany), equipment at the Centro de Microscopía Electrónica at the Universidad Nacional de Córdoba, Facultad de Ciencias Médicas.

2.13 Annexin-V-FITC/PI apoptosis assay

For apoptosis assay [27], C6 cells ($5x10^5$ cells/well) were seeded in a 6-well plate for 24 h and treated with ConBr (10, 30 and 50 µg/mL) or vehicle for 6 h. At the end of treatments, the cells were trypsinized and pooled to obtain 10^6 cells per sample. The samples were centrifuged at 1,154 x g for 5 min and the pellet suspended in 200 µL of binding buffer (10 mM HEPES, 140 mM NaCl and 25 mM CaCl2, pH 7.4) followed by incubation with 2 µL of Annexin-V-FICT (Life technology®) and 2 µL of Propidium Iodide (1mg/mL) (Sigma®) for 15 min in the dark. Staurosporin (1 µM; 3 h) treated cells were used as a positive control for Annexin-V-FITC externalization. Ten thousand events per sample were collected using a FACS Comer Device (Becton Dickson®) equipment at the Laboratório Multiusuário de Estudos em Biologia at the Universidade Federal de Santa Catarina (LAMEB/UFSC). The data were analyzed in Flowing 2.5.1® software, using FITC (515-545 nm) and PE (564-606 nm) channels for analysis of Annexin-V-FITC and Propidium Iodide, respectively.

2.14 Caspase-3 activation Assay

In order to investigate the capability of ConBr in to activate casp-3 was used of EnzChek® caspase-3 Assay Kit [27]. C6 cells were plated at a density of $5x10^5$ cells/well in 6-well plate, and treatment for 6 h with vehicle or ConBr. A positive control was performed with Staurosporine (1 µM). Two wells were subjected to the same treatment concentration and joined to obtain a final reaction of 10^6 cells. After treatment, culture medium was removed and cells trypsinized and centrifuged at 3,846 x g for 5 min, washed with 0.1 M PB and stored at -80 °C overnight to favors the cell

lysis process. Subsequently, the trader's protocol was performed. To obtain data, samples were subjected to a 1 h closed kinetic test, each reading being taken every 30 seconds, under the following conditions: 342 nm excitation, 435 nm cut-off and 446 nm emission.

2.15 Western Blot

C6 cells were seeded in a 6-well plate at the density of $25x10^4$ cells per well for 24 h. Then, the cells were treated with vehicle (control) or ConBr in serum-free DMEM for 12 h. At the end of treatments, cells were homogenized in 200 μL Stop Solution (Tris 50 mM, EDTA 2 mM, SDS 4%, pH 6.8) as previously described by Nascimento et al. [27]. Proteins extracts (30 μg/sample) were electrophoresed in 6, 10, 12% SDS-PAGE minigels and transferred onto nitrocellulose membranes using a semi-dry blotting apparatus (1.2 mA/cm^2 by 1.5 h). Transfer efficiency was confirmed by Ponceau S staining of membranes. The immunodetection of Atg7, LC3A/B, Beclin-1, pJNK (Thr183/Tyr185), JNK; pAkt (Ser473), Akt, pmTORC1(Ser2448), mTORC1, Bak, Puma, Bad, pBad (Ser112) and BNIP3 at 1:1,000 dilution; pERK1/2 (Thr202/Tyr204) at 1:5,000 dilution; ERK1/2 at 1:20,000 dilution; $p\text{-}p38^{MAPK}$ (Thr180/Tyr182) and $p38^{MAPK}$ at 1:10,000 dilution was performed by overnight incubation with the respective primary antibody diluted in Tris-buffered saline Tween 20 (TBS-T) containing 2% BSA. β-actin detection (1:2,500 dilution) was used as the loading control. Unless otherwise specified, secondary antibodies were incubated at 1:1,000 dilution. Thereafter, the membranes were washed in TBS-T and incubated for 1 h at room temperature with horseradish peroxidase (HRP)-conjugated anti-IgG-rabbit/mouse antibodies as appropriate. The bands were developed by chemiluminescence substrate (Super ECL, GE®) on the Chimidoc MP, equipment at the Laboratório Multiusuário de Estudos em Biologia at the Universidade Federal de Santa Catarina (LAMEB/UFSC). The bands and OD were captured and quantified using the Image Lab® software (Bio-Rad). The phosphorylation levels of ERK1/2, $p38^{MAPK}$, JNK, Akt and mTORC1 were quantified by densitometry and OD (optical density) ratio of phospho/total levels were calculated. The measurement of LC3 was performed by dividing the OD of each form of LC3 (I and II) by the OD of β-actin. Hence, in order to express the ratio of LC3 cleavage, normalized OD of LC3II was divided by normalized OD of LC3I. Atg7, Beclin-1, Bak, Puma, p-Bad, Bad and BNIP3 were measured by dividing OD of each protein by OD of β-actina.

2.16 Cell migration (Scratch assay)

C6 glioma cells were grown to confluence in 48-well plates ($5x10^4$ cells/well), and then a wound was introduced in each well by scraping cell layers with a P200 pipette tip. The cells were washed with PBS to remove any loosely held cells [56]. Thereafter, serum-free DMEM containing vehicle (control) or ConBr. Images were captured at 0, 24 and 48 h treatment time points by an inverted NIKON eclipse T2000-U microscope. Percentage of wound closure was calculated using Image J software.

2.17 Cell migration (Transwell assay)

Given that cell proliferation could interfere with scratch assays, we performed Transwell assays as a complementary method to assess anti-migration effects of ConBr in gliomas [27]. Briefly, the transwells were placed in a 24-well plate, and then C6 cells (5×10^4 cells suspended in 100 μL DMEM) were plated onto the top chamber. Top chamber plated cells were then treated with vehicle/control or ConBr at 30 and 50 μg/mL. Ten minutes after addition of each treatment, the bottom chamber was filled with 600 μL/well of DMEM-F12 medium supplemented with 20% FBS as a chemoattractant and incubated for additional 24 h. After, the transwells were removed, and the remaining/nonmigrated cells within the top chamber were removed with the aid of a swab. Subsequently, each transwell was stained with Crystal Violet, and the migrated cells were visualized under light microscopy and counted. The migration ratio for each treatment was compared to control/vehicle treatments (considered as 100%).

2.18 Molecular Docking Analysis of interaction of ConBr to MMP-1 glycans

Molecular docking was performed using GOLD software v. 5.5 (CDCC, Cambridge, England). Structural coordinates of ConBr was obtained from PDB under id: 4H55). MMP-1 glycans were prepared using Carbohydrate Builder server (http://glycam.org), applying the glycans structures from the work of Saarinen et al. [57]. The center of the CRD cavity and all residues in a 10 Å radius were chosen for application of the algorithm. PLANTSPLP score function [58] and the following parameters were used: population size of 100, selection pressure of 1.1, number of operations of 10,000, number of islands of 5, niche size of 2, crossover frequency of 95, number of poses of 20. Lowest energy poses were chosen by combining the docking score, hydrogen bond, ligand geometry penalties and hydrophobic interactions [59–61].

2.19 Cortical astrocytes culture

Cortical cultures of astrocytes were prepared from male newborn Wistar rats at postnatal day-0 or day-1 (P0/P1) as previously described by Nascimento et al. [30,62]. The animals were provided by the Animal Core Facility at the Federal University of Santa Catarina (UFSC). All animal procedures were approved by the Institutional Animal Care and Use Committee (CEUA/UFSC); Protocol No. 2380161216. Briefly, astrocytes were seeded in 24-well plates (3.5×10^4 cells/well) and grown to confluence (7–10 days) in DMEM-F12 (Invitrogen, Carlsbad, CA) supplemented with 10 % FBS (Cultilab, Brazil) at 37 °C in a humidified 5% CO2 and 95% O2 atmosphere. After reaching cell confluence, astrocytes were treated with ConBr (10, 30 and 50 µg/mL) or vehicle for 24 h and subsequently assayed for determination of cell viability (MTT assay), morphological changes (by optical microscopy), as well as staining with AO and PI for determination of autophagy and cell membrane damage, respectively, using the same protocols afore described.

2.20 Statistical analysis

The results were analyzed using GraphPad Prism version, 5.0 (La Jolla, California, USA). The data presented normal distribution according to the Shapiro-Wilk test ($p<0.05$) and therefore were evaluated by Analysis of Variance (One-way, Two-way ANOVA) followed by Bonferroni post-hoc test. P values less than 0.05 ($p<0.05$) were considered statistically significant.

3. Results

3.1 ConBr induces morphological changes and decreased viability in C6 cells

In order to evaluate the cytotoxic effect of ConBr in glioma cells, three different cell lines were used including: C6 glioma cells, a commercial mouse line; U87MG, a commercial human glioma cell line; GBM1, a primary cell line from human GBM. The cells were treated for 24 h with vehicle (control) or 1, 10, 30 and 50 µg/mL of lectin, and cell morphology and cell viability were assessed by light microscopy and MTT assay, respectively. ConBr induced morphological changes in all cell lines tested, which included modification from a flat to spherical round- shaped morphology. Moreover, ConBr decreased C6 and GBM1 cell viability after 24 h (Supplementary

Figure X1). Taking the aforementioned results into account, we chose the C6 glioma cells line to investigate molecular mechanisms dictating ConBr cytotoxicity.

To establish a time and concentration curve response to ConBr, C6 glioma cells were incubated for 3, 6, 12, 24 and 48 h with vehicle or lectin (1, 10, 30 and 50 μg/mL). The results showed that 30 and 50 μg/mL ConBr decreased cell viability after 12 h treatment, reaching more pronounced effects after 24 and 48 h of exposure as determined by MTT assay (Fig. 1A). ConBr toxicity was associated with LDH leakage that was detectable from 12 h of treatment with 30 and 50 μg/mL (Fig. 1B). Light microscopy analysis showed that ConBr induced changes in cell morphology, including changes from a flat to spherical round- shaped morphology, which occurred as soon as 6 h and remained for at least 48 h incubation (Fig. 1C).

We then examined whether ConBr effect on cell viability could be associated with cell death induction. For analysis of losses in cell membrane integrity, C6 cells were treated with vehicle/control or ConBr and stained with PI. Figure 1E showed that a pronounced PI staining occurred from 24 to 48 h exposure to 50 μg/mL ConBr, while lower concentrations did not show such aggressive cytotoxicity. Because ConBr cytotoxicity is only extensive in the highest concentration and after prolonged exposure to the lectin, Figure 1 date collectively indicate that both cytostatic and cytotoxic effects may account to ConBr antiglioma activity, and cytotoxicity is possibly mediated by controlled (non-necrotic) mechanisms of cell death.

3.2 ConBr antiglioma effect is dependent on tertiary/quaternary structure and carbohydrate recognition domain (CRD)

Aiming to determine whether the cytotoxic effect of ConBr was dependent upon its tridimensional structure and CRD, the lectin was submitted to either thermal denaturation or blocking of CRD with α-methyl-D-mannopyranoside. Light microscopy showed that changes in C6 cell morphology induced by native protein at 30-50 μg/mL (24 h) were partially lost by CRD blockage and completely blocked by thermal denaturation (Fig. 2A). CRD blockage also abrogated the impairment of cell viability induced by native ConBr at 30 μg/mL (Fig. 2B). Cell viability impairment induced by ConBr at 50 μg/mL occurred despite the CRD blockage. Denatured ConBr lectin exerted no cytotoxicity in C6 cells (data not shown). These results indicate that tertiary/quaternary structure is essential for ConBr cytotoxicity in glioma cells.

Moreover, the mechanism underlying cytotoxicity of mild concentrations of ConBr (30 μg/mL) seems to rely on the CRD.

3.3 ConBr decrease capacity of cell migration in C6 cells

Cellular migration/motility pathways are key drivers of infiltrative behavior of glioma *in vivo*. Scratching assays showed that ConBr induced a significant decrease in cell migration, even at low concentrations (Fig. 3A). At 24 h, ConBr treatment decreased cell culture wound closure by ~50, 70 and 90% at 1, 10 and 30-50 μg/mL concentrations, respectively. Control cells reached a complete closure of the wound within 24 h (Fig. 3A). At 48 h, 50 μg/mL of lectin retained its cytostatic effect, whereas 1, 10 and 30 μg/mL ConBr showed a lower, albeit significant, magnitude of inhibition against cell migration if compared to results obtained at the 24 h time point. It should be noted that 1 and 10 μg/mL of lectin, in contrast to 30 and 50 μg/mL, showed no cytotoxic effects, but these concentrations could inhibit cell migration, indicating that ConBr impairs glioma cells, even at noncytotoxic levels. Scratch assay results were confirmed by transwell experiments which showed that C6 cells treated for 24 h with ConBr at 30 and 50 μg/mL showed 50 and 60 % inhibition of cell migration compared with control (Fig. 3B). To assess whether the cytostatic effect of ConBr would be related to an interaction in MMP-1 glycans, molecular docking was performed (Fig. 3D). The tested glycans from MMP1 (Supplementary Figures X2 and X3) were drawn following the data found in the work of Saarinen et al. 1999 [57]. The paper indicates the presence of glycans specific to normal cells and others found only in tumor cells, there are also glycans found in both normal and malignant cells, although with changes in the frequency of appearance. As shown in Table 1, ConBr was able to interact with only 1 glycan exclusive to normal cells and 3 glycans present in both cells. On the other hand, it managed to interact favorably with most of the glycans present exclusively in tumor cells. It was observed that the interactions between the lectins and the glycans took place in an internal mannosyl residue (residues from first branch), and no interaction with residues in terminal positions have been observed (Fig. 3C-D).

3.4 ConBr modulates MAPKs and Akt pathways in C6 cells

Treatment of C6 cells with ConBr for 12 h stimulated the phosphorylation of JNKs and $p38^{MAPK}$, as shown in Figure 4B-C and 4F. JNK(p54) and JNK(p46) phosphorylation displayed ~2-fold increase in response to ConBr at 50 μg/mL, as

compared to control (Fig. 4B-C). ConBr at 30 and 50 µg/mL also provoked a 7-fold increment in $p38^{MAPK}$ phosphorylation, as compared to control cells (Fig. 4F). On the other hand, ConBr decreased the phophorylation of typical glioma survival protein kinases, ERK 1/2 (Fig. 4D-E) and Akt, in C6 cells (Fig. 4G). The effect of ConBr on p-ERK1 was more pronounced since all concentrations tested were effective in decreasing ERK1 phosphorylation (Fig. 4D) whereas 50 µg/mL ConBr suppressed Akt phophorylation (Fig. 4G). Taken together, this set of results suggests a pattern of ConBr effects upon MAPKs and Akt phosphorylation that might result in cell death induction.

3.5 Autophagy and caspase-8 promote cell death in ConBr-treated glioma cells

Next, we evaluated the possible cell death pathways triggered by ConBr in C6 cells. In order to assess apoptosis, C6 cells were stained with Annexin-V-FITC and PI and evaluated by flow cytometry. As shown in Figure 5A, only ConBr at 50 µg/mL caused an increase of 2.5% in Annexin-V-FITC+/PI- labeling and 13% in Annexin-V-FITC+/PI+. Differently, PI+ labeling was detectable in 34 and 52% of cells treated with 30 and 50 µg/mL ConBr, respectively, whereas only 5.23% of cells stained positive in control treatments. Noteworthy, this effect was accompanied by caspase-3 activation (Fig. 5B), which displayed ~2-fold increase in response to 10 µg/mL and ~3-fold increase at 30-50 µg/mL ConBr as evaluated by "EnzChek® caspase-3 Assay Kit".

We also evaluated whether 6 h treatment with ConBr could disrupt mitochondrial membrane potential and ROS production, since they are events that could be involved in the mechanism of cell death induction by ConBr. However, none significant alteration in the mitochondrial membrane potential was observed in response to ConBr, as assessed by JC-1 assay (Fig. 5D-E). Moreover, as assessed by H2DCF-DA assay, ROS levels decreased in response to ConBr (Fig. 5C). These results suggest that ConBr did not affect mitochondrial function as a possible trigger to apoptosis.

Western blot evaluation of Bak and BNIP3 in total lysates from C6 cells treated with ConBr for 12 h was performed. The results did not demonstrate alteration in Bak expression compared to control (Fig. 5F and H). However, BNIP3 displayed ~7-fold increase of expression in response to ConBr at 30 and 50 µg/mL, as compared to control (Fig. 5F and G). In order to evaluate whether activation of caspase-3 and Annexin-V-FITC labeling could be related to an extrinsic apoptotic process, as a result of lectin binding to glycan residues on death receptor, we tested the effect of caspase-8/FLICE inhibitor (1µM IETD-fmk) on ConBr cytotoxicity. Interesting, the cell viability results

demonstrated that IETD-fmk pretreatment blocked the cytotoxic effect of 30 and 50 µg/mL ConBr in C6 cells after 24 h treatment (Fig. 5I).

Acridine Orange assays are largely applied to detect acidic vesicular organelles (AVO) that occur during autophagy. We observed that ConBr treatment of C6 cells for 12 h caused a significant increment of AVO labeling from 10 to 50 µg/mL ConBr (Fig. 6A). Moreover, it is important to highlight that the increase of AVO in response to ConBr for 12 h at 10 µg/mL was not accompanied by a cytotoxic effect of the lectin in C6 cells, as shown at figure 1A. After 24 h exposure, ConBr caused a significant increment of AVO at 1 to 50 µg/mL, while after 48 h treatment only 30 and 50 µg/mL ConBr enhanced AVO frequency (Fig. 6B). Notably, this result was confirmed by transmission electron microscopy (TEM) analysis that showed small vesicles and large autophagic (arrows) containing organelles and vesicular structures in the C6 cell cytoplasm, in response to 30 µg/mL ConBr treatment for 12 h (Fig. 6C). ConBr-induced AVO formation was accompanied by decreased mTORC1 phosphorylation (Fig. 6D-E), minor changes in Beclin-1 (Fig. 6D and F) and Atg7 (Fig. 6D and G), and a 3- to 6-fold increase in cleavage of LC3I to LC3II (Fig. 6D and H), a key molecular event during autophagy, as evaluated by Western blot of total lysates from C6 cells treated for 12 h with the lectin. These responses were more significant with 30 and 50 µg/mL ConBr. Finally, to identify the role of autophagy in the lectin-induced cell death, C6 cells were co-treated with ConBr and 3-MA (2 mM) or CQ (10 µM). Results indicate that impairment of cell viability induced by 30 µg/mL ConBr were abrogated by inhibition of early steps of autophagy with 3-MA, while the effect of 50 µg/mL ConBr was partially blocked by 3-MA (Fig. 6I). Blockage of later autophagy with CQ did not cause a significant protection of the cytotoxic effect of ConBr (Fig. 6J).

To corroborate a mechanism of crosstalk between caspase-8 activation and autophagic degradation, we evaluated the response of cells to pre-treatment with 3-MA or FLICE inhibitor and subsequent co-treatment with 30 µg/mL ConBr for 12 or 24 h. It was observed by morphological analysis (Fig. 7A) and MTT assay (Fig. 7B) that the cytotoxic effect of ConBr (24 h) was abrogated by treatment with 3-MA or FLICE. Concerning the expression of apoptotic and autophagy proteins it was observed that ConBr (12 h) increased the expression of BNIP3 (Fig. 7C and 7D), Puma (Fig. 7C and 7E) and induces LC3I cleavage (Fig. 7C and 7G) with no changes in Bad (Fig. 7C and 7F). Notable, 3-MA or FLICE pre-treatment was able to block the ConBr effect (Fig. 7D, E and G). This line of evidence suggests that ConBr promotes autophagy and that

this process appears to mediate ConBr toxicity to C6 cells. Furthermore, these results suggest that there exists a crosstalk mechanism between caspase-8 activation and autophagic process induced by the lectin.

3.6 ConBr did not affect the viability of primary culture from telencephalon astrocytes

To evaluate the cytotoxic effect of ConBr in normal glial cells, primary cell cultures of astrocytes were prepared from rat telencephalon and subjected to 24 h treatment with vehicle or ConBr at 10, 30 and 50 μg/mL. Light microscopy (Fig. 8A) showed no changes in astrocyte morphology in response to ConBr. ConBr treatment also had no impact on astrocyte viability, as evaluated by MTT assay (Fig. 8B). In keeping with the above-mentioned results, PI/Hoechst staining showed no evidence of losses in cell membrane integrity in ConBr-treated astrocytes (Fig. 8C). In addition, AVO formation was also not altered by ConBr as compared to control (Fig. 8D). Taken together, these data indicate a selective effect of ConBr targeting glial tumor cells while sparing normal astrocytes.

4. Discussion

Despite the advances in oncogenomics and targeted therapeutics for a variety of cancers, GBM treatment remains a major challenge in clinical oncology. Even the most promising compounds from preclinical studies, such as EGFR as PTEN/Akt inhibitors, failed to provide survival benefits in clinical trials over the last decade [63,64]. Thus, novel compounds exhibiting tumor selectivity and efficacy to eliminate cancer cells are urgently needed. An essential first step in achieving this goal is the search for new therapeutic targets and a better understanding of the cell signaling mechanisms underlying the inhibition of cell migration and proliferation, as well as the induction of glioma cell death. In recent decades, lectins have been used as a tool for differentiation between malignant and benign tumors, especially for the ability to recognize specific glycosylation patterns, some of which are associated with the metastatic process [9,13,65,66]. In addition, it has been reported that plant lectins may directly exert antitumor effects in different cancer models [9,13,15,66]. In the last years, our group has demonstrated cytotoxic effect of different lectins isolated from the subtribe *Diocleinae,* including those purified from *Canavalia virosa* (ConV), *Canavalia*

bonariensis (CaBo), *Canavalia ensiformis* (ConA), *Dioclea lasiophylla* (DlyL), *Dioclea lasiocarpa* (DLL) and *Dioclea violacea* (DVL) in C6 and U87MG glioma cell lines [12,27–30]. Herein we extended these previous studies by showing ConBr cytotoxicity against three glioma cells lineages and, utilizing the C6 glioma cell model, we uncovered the cytotoxic mechanism and molecular signaling pathways potentially involved in the autophagic cell death triggered by ConBr.

The effect of ConBr on C6 glioma cells, U87MG and GBM1 included changes in cell morphology from a flat to spherical rounded shape, an effect that was accompanied by a decrease of cell viability in the C6 and GBM1 cells, but not in the U87MG lineage. Hence, C6 glioma cells showed to be largely sensitive to ConBr, since the lectin decreased C6 glioma cell viability by 60% at concentrations equal to, or higher than, 30 µg/mL after 12 h of treatment. Regarding these set of results, it is important to state that our previous studies showed that ConA promoted losses in C6 glioma cells viability only after 24 h of treatment [27]. Moreover, ConA produced cytotoxicity against U87MG cells only after long periods (up to 48-96 h) of treatment [30]. Noteworthy, our results concerning the activity of ConBr on U87MG cell line viability appears to be in line with this previous study.

Another aspect to be considered is related to the potency of ConBr when compared to an antiglioma drug of clinical use. Temozolomide (TMZ) is the standard chemotherapy agent used for GBM treatment [67–69], even though most of the patients frequently develop chemoresistance and succumb to the disease [70]. Hence, we establish a comparative between the cytotoxic effect of ConBr and TMZ on C6 glioma cells treated for 24 h. Notable, ConBr 30 µg/mL (300 nM) displayed an effect like TMZ 400 µM (Supplementary Figure X4), showing that the activity of ConBr on C6 cells is relevant and with magnitude comparable with a standard drug applied for GBM chemotherapy.

ConBr and ConA display high similarity of amino acid sequence and crystal structure. However, differences of biological activities have been well documented for these lectins [33,34]. Moreover, other lectins of the genre *Canavalia,* such as CaBo and ConV, showed similar effect only after 24 h treatment and at higher concentration (50-100 µg/mL) [28,29]. These data highlight that ConBr is apparently more cytotoxic to C6 cells than ConA, ConV or CaBo by its strong decrease in C6 cell viability, despite the homology of structural similarity and carbohydrate affinity. Thus, it reinforces the importance of relationships between structure and biological activity [46]. Another

fundamental aspect demonstrated in the present study showed that ConBr cytotoxicity to glioma cells depends on its three-dimensional structure and CRD (Fig. 2).

ConBr-induced decrease in cell viability by MTT assay may be the product of either cell death or decreased cell proliferation. Double staining with Hoechst/PI and LDH release assays (Fig. 1B and D) indicated that ConBr is cytotoxic owing to increased PI incorporation and LDH leakage, especially at the higher concentrations (30-50 μg/mL). Noteworthy, lower ConBr concentrations were not cytotoxic, even though decreased cell migration/proliferation was observed (Fig. 3A and B). Matrix metalloproteinases (MMPs), that in humans comprise 23 enzymes, are a family of zinc-dependent endoproteases that acts on extracellular matrix (ECM) and cell surface proteins, promoting matrix remodeling, enzyme activity regulation and release of mitogenic growth factor and bioactive molecules. Hence, MMPs represent key regulatory proteins that can control cell proliferation, migration and differentiation [71–73]. Diverse MMPs members have been implicated in tumor progression and invasiveness. Noteworthy, MMP-1, MMP-2, MMP-9 and the membrane type 1 (MT1)-MMP (also known as MMP-14) have been reported to be involved in the migratory and invasive properties, as well as malignancy grade and clinical outcome of gliomas [74,75]. MMP-1, which the expression is regulated by EGF/ERK1/2 signaling, displays a core of glycans [57,73] and is well documented for its specific role in glioma migration, invasion, and malignance grade [75–78]. Hence, the ConBr inhibition of glioma migration may be postulated to occur by the ConBr´s ability to bind glycans mainly expressed on MMP-1 present in tumoral cells (Fig. 3D). Notable, previous studies showed that ConA displays the capability to modulate other members of the metalloproteinase family, the membrane type 1 metalloproteinase (MT1-MMP/MMP-14) [79]. Hence, treatment of U87 cells with ConA promoted increment of COX-2 expression, dephosphorylation of Akt and modulation of IKK-NF-kB signaling [25], as well as activation of JAK/STAT pathway and autophagy gene transcription by mechanism apparently dependent of MT1-MMP/MMP-14 modulation [80]. In spite of all these aspects, there are no reports indicating MMP-1 modulation by lectins. Thus, the molecular docking assay performed in our study showed for the first time that a legume lectin interacts favorably with glycans of MMP-1 and ConBr obtaining better scores than ConA (data not shown). Future studies will be necessary to address the participation of MMP-1 in the mechanism of cell death or inhibition of cell migration induced by ConBr in glioma cells. Although, the present work suggests for the first time

a preferential binding of ConBr with MMP-1 glycans expressed in tumoral cells. Particularly, most of the biological activities elicited by lectins are related to their capability to bind carbohydrates/glycans which leads to a biological effect [81]. Thus, the more pronounced expression of MMP-1 in high grade glioma cells [75,82], together with preferential binding of ConBr to glycans expressed in tumoral MMP-1, may illustrate the potential of selective activity of ConBr against glioma cells rather than astrocytes or neurons.

ConBr at higher levels caused a remarkable increase in $p38^{MAPK}$ and JNKs phosphorylation and promoted inhibition of ERK1/2 and Akt phosphorylation (Fig. 4). These pathways are well documented to be associated with cell migration, as well as cell death and survival [83–86]. Indeed, it has been demonstrated that these kinases are also involved in apoptosis and autophagy modulation [8,86,87]. As example, activation of JNK was reported to activate Beclin-1 and inhibits Bcl2 [88]. Therefore, future studies addressing the participation of JNKs and $p38^{MAPK}$ in the mechanism of cell death induced by ConBr will be necessary. Taken together, our data show that ConBr triggers a series of antitumor effects and positively modulates protein kinases associated with stress and cell death and negatively modulates protein kinases associated with cell survival and proliferation.

As shown in Figure 5A, only ConBr at 50 μg/mL caused a small increase of Annexin-V-FITC labeling differently that PI labeling was detectable with 30 and 50 μg/mL ConBr, accompanied by caspase-3 activation (Fig. 5B). It is well documented that PI labeling is associated with cell death due to necrosis. However, this staining may also be related to a final process of apoptosis. In addition, fragments of apoptotic cells that are not phagocytized (common in cell cultures), due to lack of cells that perform this function in culture's microenvironment, end us suffering a type of degradation that resembles necrosis, receiving the denomination of secondary necrosis [89]. Moreover, no alteration in mitochondrial membrane potential nor significant changes in the expression of pro-apoptotic effector protein Bak was detected. While ROS production was in fact decreased by ConBr, different from the effects observed in cells treated with ConA [25,27,30,36].

Proteins of the B cell lymphoma 2 (Bcl-2) family in mammals are involved in modulation of cell survival and apoptosis, and include all proteins containing at least one of the four regions called Bcl-2 homology (BH1-4) domains. The pro-survival proteins belonging to Bcl-2 family include Bcl-2, Bcl-XL and MCL-1, all displaying

four BH domains. The pro-apoptotic proteins can be divided in two distinct groups: one that encompass Bak and Bax, which is capable to promote mitochondrial permeabilization and contain four BH domains; the second is represented by the BH3-only proteins (Bim, Puma, Bid, Bad, NOXA, Bik, HRK and BMF) that contain only the BH3 domain. The pro-apoptotic BH3-only proteins such as Bad and Puma can act as sensors of cellular stress. Indeed, they can bind and inactivate specific pro-survival proteins, such Bcl-2 and Bcl-XL, or bind directly to Bax and Bak triggering apoptosis. Moreover, anti-apoptotic members such Bcl-2 and Bcl-XL, which protect mitochondrial integrity by counteracting the pro-apoptotic proteins, can also inhibit autophagy by sequestering the autophagic protein Beclin-1, that also contains BH3 domain. Hence, in many cases activation or increased expression of BH3-only proteins, such as Puma and Bad, can induce autophagy by competitive disruption of Bcl-2/ or Bcl-XL/Beclin-1 interaction [90–93]. Moreover, Bcl-2/adenovirus E1B 19-Kda-interacting protein 3 (BNIP3), an atypical pro-apoptotic BH3-only protein, may disturb mitochondrial function. BNIP3 dimerization on the outer mitochondrial membrane in response to cellular stress has been associated with cell death and heterodimers BNIP3/Bax can promote conformational modification of Bak resulting apoptosis by intrinsic pathway [90,94]. Moreover, BNIP3 in the cytosol and mitochondrial outer membrane [94] can induce mitochondrial autophagy by interaction with autophagy protein LC3 [90]. In our study it was well evidenced that ConBr can both, induce LC3I cleavage (30 and 50 µg/mL), increment AVO formation, inhibit mTORC1 and increase expression and dimerization of BNIP3, which are events associated with autophagy. When we inhibited autophagy with 3-MA (2mM), it was observed that ConBr cytotoxicity against glioma cells decreased as evaluated by MTT assay (Fig. 6I). This finding suggests that ConBr may trigger autophagy in glioma cells as a mechanism of cell death [95,96].

Studies showed that ConA after binding to mannose moiety present in glycoproteins expressed on extracellular membranes was internalized and associated to the mitochondria surface, via clathrin-mediated endocytosis. This event was accompanied by a decrease of mitochondrial membrane potential that initiates autophagy by inductions of BNIP3, Beclin-1 and LC3II [25,97]. We observed by transmission electron microscopy (Fig. 6C) the presence of double membrane vesicles, smaller than the autophagosomes, containing material indoor that were not observed in the control cells. In spite of being uncharacterized, this finding might represent a

product of ConBr endocytosis. However, this possibility deserves to be investigated in future studies.

One interesting point in our study was to show that pre-treatment with FLICE-inhibitor abrogated the ConBr-dependent cytotoxicity (Fig. 5I). This result suggests the possibility of a cell death receptor modulated by ConBr. Notable, the receptor TRAIL-R1 (DR4) and –R2 (DR5) are glycoproteins which the signaling module leads to caspase-8/caspase-3 activation promoting cell death [98,99]. It is interesting that the lectin Moringa-G, the Gal-specific Black mulberry (*Morus nigra*) lectin, induced cleavage of caspases 8, 9, and 3 leading Jukat cells death, an effect that was hampered in cells that were deficient in caspase 8-10, caspase 9, or FADD [99]. In spite the potential modulation of TRAIL receptor by ConBr, docking assay did not show a substantial interaction of lectin with the glycans expressed on TRAIL-DR4 or –DR5 (data not shown).

Moreover, it has been also documented a crosstalk between autophagy and apoptosis, where caspase-mediated cleavage of Atg5 and Beclin-1 switches autophagy to apoptosis, while the cleavage of Atg4D results in a truncated product with increased autophagic activity, via activation of LC3 [47,101]. To investigate this mechanism, we performed pre-treatment of C6 cells with 3-MA and FLICE-inhibitor (Fig. 7). The results indicated that both inhibitors counteracted the cytotoxicity induced by ConBr, as evaluated by MTT assay, and in the same way, they also abrogated the ConBr-induced increasing of Puma, BNIP3 and LC3II immunocontent. It is documented that FLICE inhibitor can also directly bind Atg3 and impede autophagy by preventing Atg3 from binding and processing of microtubule-associated protein 1A/1B-light chain 3 (LC3) [102,103]. Taken together, the results suggest: i) ConBr promotes autophagy; ii) this process appears to mediate ConBr toxicity on C6 cells; iii) ConBr promote augmentation of some apoptotic features; iv) these events are partially dependent of autophagic pathway and caspase 8.

Finally, our results suggest that ConBr displays cancer cell selectivity, since healthy astrocytes showed no change in response to lectin treatment, while primary culture of GBM1, showed changes of cell morphology and decreased cell viability in response to ConBr treatment. Such selectivity might be attributed to expression of glycosylated targets for ConBr in cancer cells but not in health astrocytes (Fig. 8) [104]. Therefore, it is reasonable to hypothesize that selectivity of lectins to cancer cells results from their binding to altered glycans typically expressed on surface tumor cells.

5. Conclusion

Our study shows the cytotoxic effect of ConBr against C6 glioma cells, which seems to involve mechanisms dependent on caspase-8 and autophagy signaling to induce cell death. Cytostatic/antimigration effects also occurred at lower ConBr concentrations. Our working model (Fig. 9) also shows that ConBr, through interaction with glycans present in glioma cell surface targets, triggers $p38^{MAPK}$ and JNK (p46/54) activation and ERK1/2, Akt and mTORC1 inhibition. The decrease of Akt/mTORC1 pathways by ConBr may be involved in the induction of autophagy, leading to cell death.

Acknowledgments

This study was supported by: the National Council for Scientific and Technological Development (CNPq) Brazil (Projects #308449/2016-9; #439601/2018-5); CNPq/RENORBIO (Project #407945/2013-0); National Coordination for the Training and Improvement of Higher Education Personnel (CAPES) Brazil via Finance Code 001 and CAPES/MINCyT Project #249/14; Santa Catarina State Research Foundation (FAPESC/PRONEX Program-NENASC Project; #1262/2012-9). AZF, BSC, KSN and RBL are recipients of a Research Scholarship from CNPq (CNPq Research Productivity). We also acknowledge GGP and CIT from Neurochemistry 4 laboratory UFSC by support for cortical astrocytes culture. We are grateful to the Laboratório Multiusuário de Estudos em Biologia at the Universidade Federal de Santa Catarina (LAMEB/UFSC) for technical assistance. IAVW received a fellowship from CAPES Foundation, Ministry of Education of Brazil. The funding agencies had no role in study design, data collection and analysis, decision to publish, or preparation of the manuscript.

Conflict of Interest

The authors have declared that there are no conflicts of interest associated with this publication and there has been no significant financial support for this work that could have influenced its outcome.

Author Contributors:

Conception of the work: Ingrid A.V. Wolin; Benildo S. Cavada; Kyria S. Nascimento; Rodrigo B. Leal

Collection of data: Ingrid A.V. Wolin; Isabella A. Heinrich; Ana Paula M. Nascimento; Priscilla G. Welter; Liliana del V. Sosa; Ana Lucia De Paul; Lara Dias Lima; Vinicius Jose Silva Osterne; Vanir Reis Pinto-Junior; Alfeu Zanotto-Filho; Cláudia Beatriz Nedel; Kyria S. Nascimento; Benildo S. Cavada; Rodrigo B. Leal

Analysis of data: Ingrid A.V. Wolin; Isabella A. Heinrich; Ana Paula M. Nascimento; Priscilla G. Welter; Liliana del V. Sosa; Ana Lucia De Paul; Lara Dias Lima; Vinicius Jose Silva Osterne; Vanir Reis Pinto-Junior; Alfeu Zanotto-Filho; Cláudia Beatriz Nedel; Kyria S. Nascimento; Benildo S. Cavada; Rodrigo B. Leal

Writing of manuscript: Ingrid A.V. Wolin; Vanir Reis Pinto-Junior; Vinicius Jose Silva Osterne; Alfeu Zanotto-Filho; Cláudia Beatriz Nedel; Kyria S. Nascimento; Benildo S. Cavada; Rodrigo B. Leal

References

[1] D.N. Louis, A. Perry, G. Reifenberger, A. von Deimling, D. Figarella-Branger, W.K. Cavenee, H. Ohgaki, O.D. Wiestler, P. Kleihues, D.W. Ellison, The 2016 World Health Organization Classification of Tumors of the Central Nervous System: a summary, Acta Neuropathol. 131 (2016) 803–820. https://doi.org/10.1007/s00401-016-1545-1.

[2] G. Guidotti, L. Brambilla, D. Rossi, Exploring Novel Molecular Targets for the Treatment of High-Grade Astrocytomas Using Peptide Therapeutics: An Overview, Cells. 9 (2020) 490. https://doi.org/10.3390/cells9020490.

[3] E. Pawlowska, J. Szczepanska, M. Szatkowska, J. Blasiak, An interplay between senescence, apoptosis and autophagy in glioblastoma multiforme—role in pathogenesis and therapeutic perspective, Int. J. Mol. Sci. 19 (2018) 889. https://doi.org/10.3390/ijms19030889.

[4] Z. Sun, H. Xue, Y. Wei, C. Wang, R. Yu, C. Wang, S. Wang, J. Xu, M. Qian, Q. Meng, G. Li, Mucin O-glycosylating enzyme GALNT2 facilitates the malignant character of glioma by activating the EGFR/PI3K/Akt/mTOR axis, Clin. Sci. 133 (2019) 1167–1184. https://doi.org/10.1042/CS20190145.

[5] J.I. Furukawa, M. Tsuda, K. Okada, T. Kimura, J. Piao, S. Tanaka, Y. Shinohara, Comprehensive glycomics of a multistep human brain tumor model reveals

specific glycosylation patterns related to malignancy, PLoS One. 10 (2015) 1–25. https://doi.org/10.1371/journal.pone.0128300.

[6] W. Wei, Y.S. Shin, M. Xue, T. Matsutani, K. Masui, H. Yang, S. Ikegami, Y. Gu, K. Herrmann, D. Johnson, X. Ding, K. Hwang, J. Kim, J. Zhou, Y. Su, X. Li, B. Bonetti, R. Chopra, C.D. James, W.K. Cavenee, T.F. Cloughesy, P.S. Mischel, J.R. Heath, B. Gini, Single-Cell Phosphoproteomics Resolves Adaptive Signaling Dynamics and Informs Targeted Combination Therapy in Glioblastoma, Cancer Cell. 29 (2016) 563–573. https://doi.org/10.1016/j.ccell.2016.03.012.

[7] J.G. Rodrigues, M. Balmaña, J.A. Macedo, J. Poças, Â. Fernandes, J.C.M. de-Freitas-Junior, S.S. Pinho, J. Gomes, A. Magalhães, C. Gomes, S. Mereiter, C.A. Reis, Glycosylation in cancer: Selected roles in tumour progression, immune modulation and metastasis, Cell. Immunol. 333 (2018) 46–57. https://doi.org/10.1016/j.cellimm.2018.03.007.

[8] Z. Liu, Y. Luo, T.T. Zhou, W.Z. Zhang, Could plant lectins become promising anti-tumour drugs for causing autophagic cell death?, Cell Prolif. 46 (2013) 509–515. https://doi.org/10.1111/cpr.12054.

[9] Q.L. Jiang, S. Zhang, M. Tian, S.Y. Zhang, T. Xie, D.Y. Chen, Y.J. Chen, J. He, J. Liu, L. Ouyang, X. Jiang, Plant lectins, from ancient sugar-binding proteins to emerging anti-cancer drugs in apoptosis and autophagy, Cell Prolif. 48 (2015) 17–28. https://doi.org/10.1111/cpr.12155.

[10] E.J.M. Van Damme, N. Lannoo, E. Fouquaert, W.J. Peumans, The identification of inducible cytoplasmic/nuclear carbohydrate-binding proteins urges to develop novel concepts about the role of plant lectins, Glycoconj. J. 20 (2003) 449–460. https://doi.org/10.1023/B:GLYC.0000038291.67527.a5.

[11] G. Poiroux, A. Barre, E.J.M. van Damme, H. Benoist, P. Rougé, Plant lectins targeting O-glycans at the cell surface as tools for cancer diagnosis, prognosis and therapy, Int. J. Mol. Sci. 18 (2017) 1232. https://doi.org/10.3390/ijms18061232.

[12] K.S. Nascimento, M.Q. Santiago, V.R. Pinto-Junior, V.J.S. Osterne, F.W.V. Martins, A.P.M. Nascimento, I.A.V. Wolin, I.A. Heinrich, M.G.Q. Martins, M.T.L. Silva, C.F. Lossio, C.R.C. Rocha, R.B. Leal, B.S. Cavada, Structural analysis of Dioclea lasiocarpa lectin: A C6 cells apoptosis-inducing protein, Int. J. Biochem. Cell Biol. 92 (2017) 79–89. https://doi.org/10.1016/j.biocel.2017.09.014.

[13] M. Mazalovska, J.C. Kouokam, Plant-Derived Lectins as Potential Cancer Therapeutics and Diagnostic Tools, Biomed Res. Int. 2020 (2020) 1631394. https://doi.org/10.1155/2020/1631394.

[14] R.B. Leal, V.R. Pinto-Junior, V.J.S. Osterne, I.A.V. Wolin, A.P.M. Nascimento, A.H.B. Neco, D.A. Araripe, P.G. Welter, C.C. Neto, J.L.A. Correia, C.R.C. Rocha, K.S. Nascimento, B.S. Cavada, Crystal structure of DlyL, a mannose-specific lectin from Dioclea lasiophylla Mart. Ex Benth seeds that display cytotoxic effects against C6 glioma cells, Int. J. Biol. Macromol. 114 (2018) 64–76. https://doi.org/10.1016/j.ijbiomac.2018.03.080.

[15] S.K. Bhutia, P.K. Panda, N. Sinha, P.P. Praharaj, C.S. Bhol, D.P. Panigrahi, K.K. Mahapatra, S. Saha, S. Patra, S.R. Mishra, B.P. Behera, S. Patil, T.K. Maiti, Plant lectins in cancer therapeutics: Targeting apoptosis and autophagy-dependent cell death, Pharmacol. Res. 144 (2019) 8–18. https://doi.org/10.1016/j.phrs.2019.04.001.

[16] L. Esch, U. Schaffrath, An update on jacalin-like lectins and their role in plant defense, Int. J. Mol. Sci. 18 (2017) 1592. https://doi.org/10.3390/ijms18071592.

[17] B. Cavada, T. Barbosa, S. Arruda, T. Grangeiro, M. Barral-Netto, Revisiting proteus: Do Minor Changes in Lectin Structure Matter in Biological Activity? Lessons from and Potential Biotechnological Uses of the Diocleinae Subtribe Lectins, Curr. Protein Pept. Sci. 2 (2001) 123–35. https://doi.org/10.2174/1389203013381152.

[18] J.L.A. Correia, A.S.F. Do Nascimento, J.B. Cajazeiras, A.C.S. Gondim, R.I. Pereira, B.L. De Sousa, A.L.C. Da Silva, W. Garcia, E.H. Teixeira, K.S. Do Nascimento, B.A.M. Da Rocha, C.S. Nagano, A.H. Sampaio, B.S. Cavada, Molecular characterization and tandem mass spectrometry of the lectin extracted from the seeds of dioclea sclerocarpa ducke, Molecules. 16 (2011) 9077–89. https://doi.org/10.3390/molecules16119077.

[19] B.A.M. Rocha, F.B.M.B. Moreno, P. Delatorre, E.P. Souza, E.S. Marinho, R.G. Benevides, J.K.R. Rustiguel, L.A.G. Souza, C.S. Nagano, H. Debray, A.H. Sampaio, W.F. De Azevedo, B.S. Cavada, Purification, characterization, and preliminary x-ray diffraction analysis of a lactose-specific lectin from Cymbosema roseum seeds, Appl. Biochem. Biotechnol. 152 (2009) 383–93. https://doi.org/10.1007/s12010-008-8334-9.

[20] V.R. Pinto-Junior, V.J.S. Osterne, M.Q. Santiago, J.L.A. Correia, F.N. Pereira-

Junior, R.B. Leal, M.G. Pereira, L.S. Chicas, C.S. Nagano, B.A.M. Rocha, J.C. Silva-Filho, W.P. Ferreira, C.R.C. Rocha, K.S. Nascimento, A.M.S. Assreuy, B.S. Cavada, Structural studies of a vasorelaxant lectin from Dioclea reflexa Hook seeds: Crystal structure, molecular docking and dynamics, Int. J. Biol. Macromol. 98 (2017) 12–23. https://doi.org/10.1016/j.ijbiomac.2017.01.092.

[21] I. Lagarda-Diaz, A.M. Guzman-Partida, L. Vazquez-Moreno, Legume lectins: Proteins with diverse applications, Int. J. Mol. Sci. 18 (2017) 1242. https://doi.org/10.3390/ijms18061242.

[22] B. Liu, C. yang Li, H. jiao Bian, M. wei Min, L. fei Chen, J. ku Bao, Antiproliferative activity and apoptosis-inducing mechanism of Concanavalin A on human melanoma A375 cells, Arch. Biochem. Biophys. 482 (2009) 1–6. https://doi.org/10.1016/j.abb.2008.12.003.

[23] B. Liu, G.W. Min, J.K. Bao, Induction of apoptosis by concanavalin A and its molecular mechanisms in cancer cells, Autophagy. 5 (2009) 432–3. https://doi.org/10.4161/auto.5.3.7924.

[24] H.Y. Lei, C.P. Chang, Induction of autophagy by concanavalin A and its application in anti-tumor therapy, Autophagy. (2007). https://doi.org/10.4161/auto.4280.

[25] W. wen Li, J. ying Yu, H. long Xu, J. ku Bao, Concanavalin A: A potential anti-neoplastic agent targeting apoptosis, autophagy and anti-angiogenesis for cancer therapeutics, Biochem. Biophys. Res. Commun. 414 (2011) 282–286. https://doi.org/10.1016/j.bbrc.2011.09.072.

[26] C.P. Chang, M.C. Yang, H.S. Liu, Y.S. Lin, H.Y. Lei, Concanavalin A induces autophagy in hepatoma cells and has a therapeutic effect in a murine in situ hepatoma model, Hepatology. 45 (2007) 286–296. https://doi.org/10.1002/hep.21509.

[27] A.P.M. Nascimento, J.L. Knaut, D.K. Rieger, I.A.V. Wolin, I.A. Heinrich, J. Mann, A. V. Juarez, L. del V. Sosa, A.L. De Paul, C.G. Moreira, I.B. Silva, C.S. Nobre, V.J.S. Osterne, K.S. Nascimento, B.S. Cavada, R.B. Leal, Anti-glioma properties of DVL, a lectin purified from Dioclea violacea, Int. J. Biol. Macromol. 120 (2018) 566–577. https://doi.org/10.1016/j.ijbiomac.2018.08.106.

[28] V.J.S. Osterne, J.C. Silva-Filho, M.Q. Santiago, V.R. Pinto-Junior, A.C. Almeida, A.A.G.C. Barreto, I.A.V. Wolin, A.P.M. Nascimento, R.M.F. Amorim, B.A.M. Rocha, P. Delatorre, C.S. Nagano, R.B. Leal, A.M.S. Assreuy, K.S.

Nascimento, B.S. Cavada, Structural characterization of a lectin from Canavalia virosa seeds with inflammatory and cytotoxic activities, Int. J. Biol. Macromol. 94 (2017) 271–282. https://doi.org/10.1016/j.ijbiomac.2016.10.020.

[29] B.S. Cavada, M.T.L. Silva, V.J.S. Osterne, V.R. Pinto-Junior, A.P.M. Nascimento, I.A.V. Wolin, I.A. Heinrich, C.A.S. Nobre, C.G. Moreira, C.F. Lossio, C.R.C. Rocha, J.L. Martins, K.S. Nascimento, R.B. Leal, Canavalia bonariensis lectin: Molecular bases of glycoconjugates interaction and antiglioma potential, Int. J. Biol. Macromol. 106 (2018) 369–378. https://doi.org/10.1016/j.ijbiomac.2017.08.023.

[30] A.P.M. Nascimento, I.A.V. Wolin, P.G. Welter, I.A. Heinrich, A. Zanotto-Filho, V.J.S. Osterne, C.F. Lossio, M.T.L. Silva, K.S. Nascimento, B.S. Cavada, R.B. Leal, Lectin from Dioclea violacea induces autophagy in U87 glioma cells, Int. J. Biol. Macromol. 34 (2019) 660–672. https://doi.org/10.1016/j.ijbiomac.2019.04.203.

[31] T.B. Grangeiro, A. Schriefer, J.J. Calvete, M. Raida, C. Urbanke, M. Barral-Netto, B.S. Cavada, Molecular cloning and characterization of ConBr, the lectin of Canavalin brasiliensis seeds, Eur. J. Biochem. 248 (1997) 43–8. https://doi.org/10.1111/j.1432-1033.1997.00043.x.

[32] B.S. Cavada, V.J.S. Osterne, C.F. Lossio, V.R. Pinto-Junior, M.V. Oliveira, M.T.L. Silva, R.B. Leal, K.S. Nascimento, One century of ConA and 40 years of ConBr research: A structural review, Int. J. Biol. Macromol. 134 (2019) 901–911. https://doi.org/10.1016/j.ijbiomac.2019.05.100.

[33] B.S. Cavada, V.J.S. Osterne, V.R. Pinto-Junior, K.S. Nascimento, ConBr, the Lectin from Canavalia brasiliensis Mart. Seeds: Forty Years of Research, Curr. Protein Pept. Sci. 20 (2019) 600–613. https://doi.org/10.2174/1389203720666190104123210.

[34] B.S. Cavada, V.R. Pinto-Junior, V.J.S. Osterne, K.S. Nascimento, ConA-like lectins: High similarity proteins as models to study structure/biological activities relationships, Int. J. Mol. Sci. 20 (2019) 30. https://doi.org/10.3390/ijms20010030.

[35] J.E.C. Batista, M.T. Ralph, R. V. Vaz, P.F.C. Souza, A.B. Silva, D.C.O. Nascimento, L.T. Souza, M. V. Ramos, P. Mastroeni, J. V. Lima-Filho, Plant lectins ConBr and CFL modulate expression toll-like receptors, pro-inflammatory cytokines and reduce the bacterial burden in macrophages infected with

Salmonella enterica serovar Typhimurium, Phytomedicine. 25 (2017) 52–60. https://doi.org/10.1016/j.phymed.2016.12.005.

[36] G. V. Faheina-Martins, A.L. da Silveira, B.C. Cavalcanti, M. V. Ramos, M.O. Moraes, C. Pessoa, D.A.M. Araújo, Antiproliferative effects of lectins from Canavalia ensiformis and Canavalia brasiliensis in human leukemia cell lines, Toxicol. Vitr. 26 (2012) 1161–1169. https://doi.org/10.1016/j.tiv.2012.06.017.

[37] F. de O. Silva, P. das N. Santos, E. de O. FigueirÔa, C.M.L. de Melo, J.K. de Andrade Lemoine Neves, F.V.S. Arruda, J.B. Cajazeiras, K.S. do Nascimento, E.H. Teixeira, B.S. Cavada, A.L.F. Porto, V.R.A. Pereira, Antiproliferative effect of Canavalia brasiliensis lectin on B16F10 cells, Res. Vet. Sci. 96 (2014) 276–82. https://doi.org/10.1016/j.rvsc.2014.01.005.

[38] S.C. Barauna, M.P. Kaster, B.T. Heckert, K.S. do Nascimento, F.M. Rossi, E.H. Teixeira, B.S. Cavada, A.L.S. Rodrigues, R.B. Leal, Antidepressant-like effect of lectin from Canavalia brasiliensis (ConBr) administered centrally in mice, Pharmacol. Biochem. Behav. 85 (2006) 160–169. https://doi.org/10.1016/j.pbb.2006.07.030.

[39] M.A. Russi, S. Vandresen-Filho, D.K. Rieger, A.P. Costa, M.W. Lopes, R.M.S. Cunha, E.H. Teixeira, K.S. Nascimento, B.S. Cavada, C.I. Tasca, R.B. Leal, ConBr, a lectin from canavalia brasiliensis seeds, protects against quinolinic acid-induced seizures in mice, Neurochem. Res. 37 (2012) 288–297. https://doi.org/10.1007/s11064-011-0608-x.

[40] D.K. Rieger, A.P. Costa, J. Budni, M. Moretti, S.G.R. Barbosa, K.S. Nascimento, E.H. Teixeira, B.S. Cavada, A.L.S. Rodrigues, R.B. Leal, Antidepressant-like effect of Canavalia brasiliensis (ConBr) lectin in mice: Evidence for the involvement of the glutamatergic system, Pharmacol. Biochem. Behav. 122 (2014) 53–60. https://doi.org/10.1016/j.pbb.2014.03.008.

[41] D.K. Rieger, R.M.S. Cunha, M.W. Lopes, A.P. Costa, J. Budni, A.L.S. Rodrigues, R. Walz, E.H. Teixeira, K.S. Nascimento, B.S. Cavada, R.B. Leal, ConBr, a lectin from Canavalia brasiliensis seeds, modulates signaling pathways and increases BDNF expression probably via a glycosylated target, J. Mol. Recognit. 27 (2014) 746–754. https://doi.org/10.1002/jmr.2401.

[42] A. V. Jacques, D.K. Rieger, M. Maestri, M.W. Lopes, T. V. Peres, F.M. Gonçalves, D.Z. Pedro, C.I. Tasca, M.G. López, J. Egea, K.S. Nascimento, B.S. Cavada, R.B. Leal, Lectin from Canavalia brasiliensis (ConBr) protects

hippocampal slices against glutamate neurotoxicity in a manner dependent of PI3K/Akt pathway, Neurochem. Int. 62 (2013) 836–842. https://doi.org/10.1016/j.neuint.2013.02.020.

[43] D.K. Rieger, E. Navarro, I. Buendia, E. Parada, L. González-Lafuente, R. Leon, A.P. Costa, I.A. Heinrich, K.S. Nascimento, B.S. Cavada, M.G. Lopez, J. Egea, R.B. Leal, ConBr, A Lectin Purified from the Seeds of Canavalia brasiliensis, Protects Against Ischemia in Organotypic Culture of Rat Hippocampus: Potential Implication of Voltage-Gated Calcium Channels, Neurochem. Res. 42 (2017) 347–359. https://doi.org/10.1007/s11064-016-2078-7.

[44] R.A. Moreira, B.S. Gavada, Lectin from Canavalia brasiliensis (MART.). isolation, characterization and behavior during germination, Biol. Plant. 13 (1984). https://doi.org/10.1007/BF02902274.

[45] L.F.F. Bittencourt, K.A. Oliveira, C.B. Cardoso, F.G. Lopes, T. Dal-Cim, L.D. Chiaradia-Delatorre, A. Mascarello, S.W. Maluf, R.A. Yunes, R.C. Garcez, C.I. Tasca, C.B. Nedel, Novel synthetic chalcones induces apoptosis in human glioblastoma cells, Chemico-Biological Interactions 252 (2016) 74-81. http://dx.doi.org/10.1016/j.cbi.2016.03.022

[46] R. Bortul, P.L. Tazzari, A. Cappellini, G. Tabellini, A.M. Billi, R. Bareggi, L. Manzoli, L. Cocco, A.M. Martelli, Constitutively active Akt1 protects HL60 leukemia cells from TRAIL-induced apoptosis through a mechanism involving NF-κB activation and cFLIPL up-regulation, Leukemia. 17 (2003) 379–389. https://doi.org/10.1038/sj.leu.2402793.

[47] W. Hou, J. Han, C. Lu, L.A. Goldstein, H. Rabinowich, A crosstalk mechanism between autophagy and apoptosis Autophagic degradation of active caspase-8, (2010) 891–900. https://doi.org/10.4161/auto.6.7.13038.

[48] X. Zhang, W. Li, C. Wang, X. Leng, S. Lian, J. Feng, J. Li, H. Wang, Inhibition of autophagy enhances apoptosis induced by proteasome inhibitor bortezomib in human glioblastoma U87 and U251 cells, Mol. Cell. Biochem. 385 (2014) 265–275. https://doi.org/10.1007/s11010-013-1835-z.

[49] H. Ye, M. Chen, F. Cao, H. Huang, R. Zhan, X. Zheng, Chloroquine, an autophagy inhibitor, potentiates the radiosensitivity of glioma initiating cells by inhibiting autophagy and activating apoptosis, BMC Neurol. 16 (2016) 1–8. https://doi.org/10.1186/s12883-016-0700-6.

[50] M. Mauthe, I. Orhon, C. Rocchi, X. Zhou, M. Luhr, K.J. Hijlkema, R.P. Coppes,

N. Engedal, M. Mari, F. Reggiori, Chloroquine inhibits autophagic flux by decreasing autophagosome-lysosome fusion, Autophagy. 14 (2018) 1435–1455. https://doi.org/10.1080/15548627.2018.1474314.

[51] T. Mosmann, Rapid colorimetric assay for cellular growth and survival: Application to proliferation and cytotoxicity assays, J. Immunol. Methods. 65 (1983) 55–63. https://doi.org/10.1016/0022-1759(83)90303-4.

[52] R. Rosa, C. Sanfeliu, E. Rodríguez-Farré, A. Frandsen, A. Schousboe, C. Suñol, Properties of ryanodine receptors in cultured cerebellar granule neurons: Effects of hexachlorocyclohexane isomers and calcium, J. Neurosci. Res. 47 (1997) 27–33. https://doi.org/10.1002/(SICI)1097-4547(19970101)47:1<27::AID-JNR3>3.0.CO;2-H.

[53] S. De Biasi, L. Gibellini, A. Cossarizza, Uncompensated polychromatic analysis of mitochondrial membrane potential using JC-1 and multilaser excitation, Curr. Protoc. Cytom. 2015 (2015) 7.32.1-7.32.11. https://doi.org/10.1002/0471142956.cy0732s72.

[54] R. Singh, L. Nawale, D. Sarkar, C.G. Suresh, Two chitotriose-specific lectins show anti-angiogenesis, induces caspase-9-mediated apoptosis and early arrest of pancreatic tumor cell cycle, PLoS One. 11 (2016) 1–18. https://doi.org/10.1371/journal.pone.0146110.

[55] A.L. De Paul, A.M. Attademo, R.W. Carón, M. Soaje, A.I. Torres, G.A. Jahn, M.E. Celis, Neuropeptide glutamic-isoleucine (NEI) specifically stimulates the secretory activity of gonadotrophs in primary cultures of female rat pituitary cells, Peptides. 30 (2009) 2081–7. https://doi.org/10.1016/j.peptides.2009.08.022.

[56] C.C. Liang, A.Y. Park, J.L. Guan, In vitro scratch assay: A convenient and inexpensive method for analysis of cell migration in vitro, Nat. Protoc. 2 (2007) 329–33. https://doi.org/10.1038/nprot.2007.30.

[57] J. Saarinen, H.G. Welgus, C.A. Flizar, N. Kalkkinen, J. Helin, N-Glycan structures of matrix metalloproteinase-1 derived from human fibroblasts and from HT-1080 fibrosarcoma cells, Eur. J. Biochem. 259 (1999) 829–840.

[58] O. Korb, T. Stützle, T.E. Exner, Empirical scoring functions for advanced Protein-Ligand docking with PLANTS, J. Chem. Inf. Model. 49 (2009) 84–96. https://doi.org/10.1021/ci800298z.

[59] M.B. de Ávila, M.M. Xavier, V.O. Pintro, W.F. de Azevedo, Supervised machine learning techniques to predict binding affinity. A study for cyclin-dependent

kinase 2, Biochem. Biophys. Res. Commun. 494 (2017) 305–310. https://doi.org/10.1016/j.bbrc.2017.10.035.

[60] G.S. Heck, V.O. Pintro, R.R. Pereira, M.B. de Ávila, N.M.B. Levin, W.F. de Azevedo, Supervised Machine Learning Methods Applied to Predict Ligand-Binding Affinity, Curr. Med. Chem. 24 (2017) 2459–2470. https://doi.org/10.2174/0929867324666170623092503.

[61] M.M. Xavier, G.S. Heck, M.B. de Avila, N.M.B. Levin, V.O. Pintro, N.L. Carvalho, W.F. de Azevedo, SAnDReS a Computational Tool for Statistical Analysis of Docking Results and Development of Scoring Functions, Comb. Chem. High Throughput Screen. 19 (2016) 801–812. https://doi.org/10.2174/1386207319666160927111347.

[62] T. Dal-Cim, G.G. Poluceno, D. Lanznaster, K.A. de Oliveira, C.B. Nedel, C.I. Tasca, Guanosine prevents oxidative damage and glutamate uptake impairment induced by oxygen/glucose deprivation in cortical astrocyte cultures: involvement of A1 and A2A adenosine receptors and PI3K, MEK, and PKC pathways, Purinergic Signal. 15 (2019) 465–476. https://doi.org/10.1007/s11302-019-09679-w.

[63] S.Y. Hwang, S. Park, Y. Kwon, Recent therapeutic trends and promising targets in triple negative breast cancer, Pharmacol. Ther. 199 (2019) 30–57. https://doi.org/10.1016/j.pharmthera.2019.02.006.

[64] Q. Fan, C.K. Cheng, T.P. Nicolaides, A. Zachary, K.M. Shokat, W.A. Weiss, A dual PI3K α/mTOR inhibitor cooperates with blockade of EGFR in PTEN-mutant glioma, Cancer Res. J. 67 (2008) 7960–7965. https://doi.org/10.1158/0008-5472.CAN-07-2154.A.

[65] T. Yau, X. Dan, C.C.W. Ng, T.B. Ng, Lectins with potential for anti-cancer therapy, Molecules. 20 (2015) 3791–3810. https://doi.org/10.3390/molecules20033791.

[66] H. Mao, D.G. Lebrun, J. Yang, V.F. Zhu, M. Li, Deregulated signaling pathways in glioblastoma multiforme: Molecular mechanisms and therapeutic targets, Cancer Invest. 30 (2012) 48–56. https://doi.org/10.3109/07357907.2011.630050.

[67] B.J. Theeler, M.R. Gilbert, Advances in the treatment of newly diagnosed glioblastoma, BMC Med. 13 (2015) 1–11. https://doi.org/10.1186/s12916-015-0536-8.

[68] B.K. Shah, A. Bista, S. Sharma, Survival trends in elderly patients with

glioblastoma in the United States: A population-based study, Anticancer Res. 36 (2016) 4883–6. https://doi.org/10.21873/anticanres.11052.

[69] E. Ozdemir-Kaynak, A.A. Qutub, O. Yesil-Celiktas, Advances in glioblastoma multiforme treatment: New models for nanoparticle therapy, Front. Physiol. 9 (2018) 170. https://doi.org/10.3389/fphys.2018.00170.

[70] S.Y. Lee, Temozolomide resistance in glioblastoma multiforme, Genes Dis. 3 (2016) 198–210. https://doi.org/10.1016/j.gendis.2016.04.007.

[71] N. Cui, M. Hu, R.A. Khalil, Biochemical and Biological Attributes of Matrix Metalloproteinases, in: Prog. Mol. Biol. Transl. Sci., 2017: pp. 1–73. https://doi.org/10.1016/bs.pmbts.2017.02.005.

[72] M. Levin, Y. Udi, I. Solomonov, I. Sagi, Next generation matrix metalloproteinase inhibitors — Novel strategies bring new prospects, Biochim. Biophys. Acta - Mol. Cell Res. 1864 (2017) 1927–1939. https://doi.org/10.1016/j.bbamcr.2017.06.009.

[73] M.S. Ågren, U. Auf Dem Keller, Matrix metalloproteinases: How much can they do?, Int. J. Mol. Sci. 21 (2020) 1–9. https://doi.org/10.3390/ijms21082678.

[74] C. Hagemann, A complete compilation of matrix metalloproteinase expression in human malignant gliomas, World J. Clin. Oncol. 3 (2012) 67–79. https://doi.org/10.5306/wjco.v3.i5.67.

[75] J. Stojic, C. Hagemann, S. Haas, C. Herbold, S. Kühnel, S. Gerngras, W. Roggendorf, K. Roosen, G.H. Vince, Expression of matrix metalloproteinases MMP-1, MMP-11 and MMP-19 is correlated with the WHO-grading of human malignant gliomas, Neurosci. Res. 60 (2008) 40–9. https://doi.org/10.1016/j.neures.2007.09.009.

[76] P. Kunapuli, C.S. Kasyapa, L. Hawthorn, J.K. Cowell, LGI1, a putative tumor metastasis suppressor gene, controls in Vitro invasiveness and expression of matrix metalloproteinases in glioma cells through the ERK1/2 pathway, J. Biol. Chem. 279 (2004) 23151–23157. https://doi.org/10.1074/jbc.M314192200.

[77] M. Anand, T.E. Van Meter, H.L. Fillmore, Epidermal growth factor induces matrix metalloproteinase-1 (MMP-1) expression and invasion in glioma cell lines via the MAPK pathway, J. Neurooncol. 104 (2011) 679–87. https://doi.org/10.1007/s11060-011-0549-x.

[78] J.N. Tung, C.P. Ko, S.F. Yang, C.W. Cheng, P.N. Chen, C.Y. Chang, C.L. Lin, T.F. Yang, Y.H. Hsieh, K.C. Chen, Inhibition of pentraxin 3 in glioma cells

impairs proliferation and invasion in vitro and in vivo, J. Neurooncol. 129 (2016) 201–9. https://doi.org/10.1007/s11060-016-2168-z.

[79] N. Akla, J. Pratt, B. Annabi, Concanavalin-A triggers inflammatory response through JAK/STAT3 signalling and modulates MT1-MMP regulation of COX-2 in mesenchymal stromal cells, Exp. Cell Res. 318 (2012) 2498–2506. https://doi.org/10.1016/j.yexcr.2012.08.003.

[80] J. Pratt, B. Annabi, Induction of autophagy biomarker BNIP3 requires a JAK2/STAT3 and MT1-MMP signaling interplay in Concanavalin-A-activated U87 glioblastoma cells, Cell. Signal. 26 (2014) 917–924. https://doi.org/10.1016/j.cellsig.2014.01.012.

[81] G.F.O. Marques, V.J.S. Osterne, L.M. Almeida, M. V. Oliveira, L.A.C. Brizeno, V.R. Pinto-Junior, M.Q. Santiago, A.H.B. Neco, M.R.L. Mota, L.A.G. Souza, K.S. Nascimento, A.F. Pires, B.S. Cavada, A.M.S. Assreuy, Contribution of the carbohydrate-binding ability of Vatairea guianensis lectin to induce edematogenic activity, Biochimie. 140 (2017) 58–65. https://doi.org/10.1016/j.biochi.2017.06.008.

[82] Y. Zhang, H. Zhan, W. Xu, Z. Yuan, P. Lu, L. Zhan, Q. Li, Upregulation of matrix metalloproteinase-1 and proteinase-activated receptor-1 promotes the progression of human gliomas, Pathol. Res. Pract. 207 (2011) 24–9. https://doi.org/10.1016/j.prp.2010.10.003.

[83] T. Ersahin, N. Tuncbag, R. Cetin-Atalay, The PI3K/AKT/mTOR interactive pathway, Mol. Biosyst. 11 (2015) 1946–54. https://doi.org/10.1039/c5mb00101c.

[84] S. Shen, Y. Zhang, R. Zhang, X. Tu, X. Gong, Ursolic acid induces autophagy in U87MG cells via ROS-dependent endoplasmic reticulum stress, Chem. Biol. Interact. 218 (2014) 28–41. https://doi.org/10.1016/j.cbi.2014.04.017.

[85] T. Zarubin, J. Han, Activation and signaling of the p38 MAP kinase pathway, Cell Res. 15 (2005) 11–8. https://doi.org/10.1038/sj.cr.7290257.

[86] Z. Li, X. Zhang, Kinases involved in both autophagy and mitosis, Int. J. Mol. Sci. 18 (2017) 1–15. https://doi.org/10.3390/ijms18091884.

[87] F. Song, Y. Wang, D. Jiang, T. Wang, Y. Zhang, H. Ma, Y. Kang, Cyclic compressive stress regulates apoptosis in rat osteoblasts: Involvement of PI3K/Akt and JNK MAPK Signaling pathways, PLoS One. 11 (2016) 1–16. https://doi.org/10.1371/journal.pone.0165845.

[88] Y. Wei, S. Pattingre, S. Sinha, M. Bassik, B. Levine, JNK1-Mediated

Phosphorylation of Bcl-2 Regulates Starvation-Induced Autophagy, Mol. Cell. 30 (2008) 678–88. https://doi.org/10.1016/j.molcel.2008.06.001.

[89] U. Ziegler, P. Groscurth, Morphological features of cell death, News Physiol. Sci. 19 (2004) 124–8. https://doi.org/10.1152/nips.01519.2004.

[90] S. Rikka, M.N. Quinsay, R.L. Thomas, D.A. Kubli, X. Zhang, A.N. Murphy, Å. Gustafsson, Bnip3 impairs mitochondrial bioenergetics and stimulates mitochondrial turnover, Cell Death Differ. 18 (2011) 721–731. https://doi.org/10.1038/cdd.2010.146.

[91] S. Cory, J.M. Adams, The BCL2 family: Regulators of the cellular life-or-death switch, Nat. Rev. Cancer. 2 (2002) 647–656. https://doi.org/10.1038/nrc883.

[92] D. Westphal, G. Dewson, P.E. Czabotar, R.M. Kluck, Molecular biology of Bax and Bak activation and action, Biochim. Biophys. Acta - Mol. Cell Res. 1813 (2011) 521–531. https://doi.org/10.1016/j.bbamcr.2010.12.019.

[93] P. Bhat, J. Kriel, B. Shubha Priya, Basappa, N.S. Shivananju, B. Loos, Modulating autophagy in cancer therapy: Advancements and challenges for cancer cell death sensitization, Biochem. Pharmacol. 147 (2018) 170–182. https://doi.org/10.1016/j.bcp.2017.11.021.

[94] U.B. Hendgen-Cotta, S. Esfeld, K. Rudi, I. Miinalainen, J.P. Klare, T. Rassaf, Cytosolic BNIP3 dimer interacts with mitochondrial bax forming heterodimers in the mitochondrial outer membrane under basal conditions, Int. J. Mol. Sci. 18 (2017) 1–15. https://doi.org/10.3390/ijms18040687.

[95] T. Kanzawa, I.M. Germano, T. Komata, H. Ito, Y. Kondo, S. Kondo, Role of autophagy in temozolomide-induced cytotoxicity for malignant glioma cells, Cell Death Differ. 11 (2004) 448–457. https://doi.org/10.1038/sj.cdd.4401359.

[96] Z.J. Yang, C.E. Chee, S. Huang, F.A. Sinicrope, The role of autophagy in cancer: Therapeutic implications, Mol. Cancer Ther. 10 (2011) 1533–41. https://doi.org/10.1158/1535-7163.MCT-11-0047.

[97] J. Pratt, R. Roy, B. Annabi, Concanavalin-A-induced autophagy biomarkers requires membrane type-1 matrix metalloproteinase intracellular signaling in glioblastoma cells, Glycobiology. 22 (2012) 1245–1255. https://doi.org/10.1093/glycob/cws093.

[98] O. Micheau, Regulation of TNF-related apoptosis-inducing ligand signaling by glycosylation, Int. J. Mol. Sci. 19 (2018) 715. https://doi.org/10.3390/ijms19030715.

[99] O. Aktas, U. Schulze-Topphoff, F. Zipp, T. Griffith, B. Stokes, T. Kucaba, J. Earel Jr., R. VanOosten, E. Brincks, L. Norian, TRAIL Gene Therapy: From Preclinical Development to Clinical Application, Curr. Gene Ther. 12 (2007) 2912–2921. https://doi.org/10.2174/156652309787354612.

[100] G. Poiroux, A. Barre, M. Simplicien, S. Pelofy, S. Bruno, E.J.M. Van Damme, P. Roug, H. Benoist, Morniga-G , a T / Tn-Specific Lectin , Induces Leukemic Cell Death via Caspase and DR5 Receptor-Dependent Pathways, Int. J. Mol. Sci. 20 (2019) 230. https://doi.org/10.3390/ijms20010230.

[101] J.O. Pyo, M.H. Jang, Y.K. Kwon, H.J. Lee, J. Il Jun, H.N. Woo, D.H. Cho, B.Y. Choi, H. Lee, J.H. Kim, N. Mizushima, Y. Oshumi, Y.K. Jung, Essential roles of Atg5 and FADD in autophagic cell death: Dissection of autophagic cell death into vacuole formation and cell death, J. Biol. Chem. 280 (2005) 20722–9. https://doi.org/10.1074/jbc.M413934200.

[102] J.S. Lee, Q. Li, J.Y. Lee, S.H. Lee, J.H. Jeong, H.R. Lee, H. Chang, F.C. Zhou, S.J. Gao, C. Liang, J.U. Jung, FLIP-mediated autophagy regulation in cell death control, Nat. Cell Biol. 11 (2009) 1355–62. https://doi.org/10.1038/ncb1980.

[103] P. Smyth, T. Sessler, C.J. Scott, D.B. Longley, FLIP(L): the pseudo-caspase, FEBS J. (2020) 1–15. https://doi.org/10.1111/febs.15260.

[104] R.G. Lichtenstein, G.A. Rabinovich, Glycobiology of cell death: When glycans and lectins govern cell fate, Cell Death Differ. 20 (2013) 976–986. https://doi.org/10.1038/cdd.2013.50.

Figure Legends

Figure 1. ConBr decreases cell viability in C6 glioma cell. C6 glioma cells were treated for 3, 6, 12, 24 and 48 h with vehicle (HEPES-saline buffer; control) or 1, 10, 30 and 50 µg/mL ConBr. Thereafter, cell morphology, cell viability and PI incorporation assays were performed. **A)** MTT cell viability assay after ConBr treatment. **B)** LDH assay after 12 and 24 h of ConBr treatment. **C)** Representative images of cell morphology alterations in response to ConBr treatment. **D)** Representative images comparing effect of ConBr at 10 and 50 µg/mL compared to control for 6 and 24 h of treatment and **E)** quantification of PI staining in response to ConBr treatment for 3, 6, 12, 24 and 48 h. The scale bar represents 50 µm. Four independent experiments were performed in triplicate. Data quantification expressed as a percentage of control (considered 100%), and the values are presented as mean ± SEM. * $p<0.05$, ** $p<0.01$ and *** $p<0.001$, as compared to control. One-way or Two-way ANOVA when appropriate followed by the Bonferroni post-hoc test

Figure 2. ConBr cytotoxicity relies on three-dimensional structure and carbohydrate-recognition domain. C6 glioma cells were treated for 24 h with vehicle or denatured/native/blocked ConBr. **A)** Representative microphotographs of cell morphology alterations in response to ConBr treatment. The scale bar represents 100 µm. **B)** MTT cell viability assay after ConBr treatment. Four independent experiments were performed in triplicate. Data quantification expressed as a percentage of control (considered 100%), and the values are presented as mean ± SEM. ** $p<0.01$ and *** $p<0.001$, as compared to control. ## $p<0.01$ as compared to treatment. Two-way ANOVA followed by the Bonferroni post-hoc test.

Figure 3. ConBr decreases cell migration in C6 cell and might interact with MMP-1 glycans. A) Effect of ConBr at 1, 10, 30 and 50 µg/mL on C6 glioma cell migration at different treatment endpoints. The scale bar represents 200 µm. The graphs show the magnitude of cell migration inhibition by lectins. **B)** Representative image of cell migration/invasion in transwell assay as assessed by inverted microscopy. The scale bar represents 200 µm. The graphs show the magnitude of cell migration inhibition by lectins. ** $p<0.01$ and *** $p<0.001$, as compared to control. ## $p<0.01$ and ### $p<0.001$ as compared to treatment. One-way or Two-way ANOVA when appropriate

followed by the Bonferroni post-hoc test. **C)** MMP-1 glycan (T012) present in tumor cells. **D)** Interaction between ConBr (green) and MMP-1 (brown) via glycosylation (yellow; T012), in cartoon representation.

Figure 4. ConBr increased JNKp46/p54 and p38^{MAPK} phosphorylation and decreased ERK1/2 and Akt phosphorylation. **A)** Representative Western blot of tested proteins and quantification of phospho- and total **B)** JNKp54, **C)** JNKp46, **D)** ERK1, **E)** ERK2, **F)** p38^{MAPK} and **G)** Akt. The phosphorylation level of each protein was determined by the ratio of the O.D. of the phosphorylated band over the O.D. of the total band. * $p<0.05$, ** $p<0.01$, *** $p<0.001$ as compared to control. One-way ANOVA followed by the Bonferroni post-hoc test.

Figure 5. ConBr effects upon apoptosis and mitochondrial function markers. A) Dot plot representation of flow cytometry of C6 cells treated with ConBr for 6 h (10,000 events per sample are shown). **B)** Caspase-3 activity assay in C6 cells treated for 6 h with varying concentrations of ConBr. **C)** ROS production after 6 h of treatment with vehicle or ConBr. **D)** Representative images comparing effect of ConBr at 50 µg/mL compared to control and **E)** quantification of mitochondrial membrane potential as evaluated by JC-1 assay in C6 cells treated for 6 h. **F)** Representative Western blot of proteins and densitometry quantification of **G)** BNIP3 and **H)** Bak protein. **I)** Effect of FLICE/caspase-8-inhibitor (2 µM) on cell viability of C6 cells treated for 24 h with ConBr as assessed by MTT assay. Data are expressed as a percentage of control (considered 100%), and the values are presented as mean ± SEM. For all analyses, four independent experiments were performed. * $p<0.05$, ** $p<0.01$ and *** $p<0.001$, as compared to control. # $p< 0.05$ and ### $p<0.001$ as compared to treatment. One-way or Two-way ANOVA when appropriate followed by the Bonferroni post-hoc test

Figure 6. ConBr treatment induces autophagy-mediated death cell. A) Representative Acridine Orange (AO) staining images of 10 and 50 µg/mL ConBr treatments for 12 and 24 h and **B)** quantification of AO staining in response to ConBr at various time points (3, 6, 12, 24 and 48 h). Chromatin (CR) and acidic vesicle organelles (AVO) were detected in green and red channels, respectively. The scale bar represents 100 µm. **C)** TEM microscopy of C6 cells treated with 30 µg/mL ConBr or vehicle for 12 h. Arrows show membrane-bound vacuoles characteristic of

autophagosomes (Magnification of 6,000 x). **D)** Representative Western blot of proteins and quantification of **E)** phospho- and total-mTORC1, **F)** Beclin-1, **G)** Atg-7 and **H)** LC3 proteins in C6 cells treated for 12 h with ConBr. **I)** Effect of 3-MA (2 mM) and **J)** CQ (10 µM) on cell viability of C6 cells submitted to lectin treatment as evaluated by MTT assay. Data are expressed as a percentage of control (considered 100%), and the values are presented as mean ± SEM. For all analyses, four independent experiments were performed. * $p<0.05$, ** $p<0.01$ and *** $p<0.001$, as compared to control. # $p< 0.05$ and ### $p<0.001$ as compared to treatment. One-way or Two-way ANOVA when appropriate followed by the Bonferroni post-hoc test.

Figure 7. ConBr treatment yield crosstalk mechanism between activate caspase-8 and autophagic degradation. C6 cells were treated for 6 h with 2 µM of FLICE inhibitor or 2 mM 3-MA for 1 h (as pretreatment of cells), and cells were co-incubated with 30 µg/mL ConBr for 12 or 24 h. **A)** Representative microphotographs of C6 cells morphology alterations in response to treatment (24 h). **B)** MTT cell viability assay performed 24 h after ConBr treatment in the presence/absence of 3-MA and FLICE inhibitor. **C)** Representative Western blot and densitometry quantification of **D)** BNIP3, **E)** Puma, **F)** Bad and **G)** LC3 proteins. Four independent experiments were performed. Quantification of data is expressed as a percentage of control (considered 100%), and the values are presented as mean ± SEM. ** $p<0.01$ and *** $p<0.001$, as compared to control. # $p< 0.05$, ## $p<0.01$ and ### $p<0.001$ as compared co-treatment (inhibitor/ConBr) to 30µg/mL ConBr. One-way or Two-way ANOVA when appropriate followed by the Bonferroni post-hoc test

Figure 8. ConBr treatment does not alter viability of primary astrocytes. A) Representative optical microscopy images of astrocytes in culture after 24 h treatment with different ConBr concentrations. The scale bar represents 100 µm. **B)** MTT cell viability in response to ConBr treatment (24 h). **C)** Representative images of Hoechst/PI and **D)** Acridine Orange staining of astrocytes after 24 h ConBr exposure. The scale bar represents 100 µm. For all analyses, four independent experiments were performed. One-way ANOVA followed by the Bonferroni post-hoc test.

Figure 9. Schematic overview of ConBr effects on C6 glioma cells. ConBr binding on glycans residues (glycose/mannose) present in the surface of C6 glioma cell induces

decrease of cell viability with increasing $p38^{MAPK}$ and JNK (p46/54) phosphorylation. This effect is accompanied by decrease of ERK1/2 and Akt activity, as well as inhibition of cell migration and cell survival. Noteworthy, the inhibition of Akt/mTORC1 pathway by ConBr may be associated with activation of autophagic processes, with cleavage of LC3 leading to cell death and apparently inhibiting mitochondrial ROS production. This complex anti-glioma activity of ConBr, might involve crosstalk mechanisms involving caspase-8 and autophagic pathways leading glioma cell death. This figure was produced using Servier Medical Art (http://www.servier.com).

Table 1. Molecular docking scores between ConBr and glycans found in MMP-1.

MMP-1 glycans	Docking score
Normal cells	
N001[a]	-48.25
N002[b]	-48.07
N003[b]	-58.88
N004[b]	-67.52
N005	-
N006	-
N007	-
N008	-
N009	-
N010	-
N011	-
Tumor cells	
T001	-63.85
T002	-67.14
T003	-67.41
T004	-43.24
T005	-42.38
T006	-48.02
T007	-
T008	-60.78
T009	-64.09
T010	-61.07
T011	-55.41
T012	-50.54
T013	-49.99
T014	-59.65
T015	-62.11
T016	-61.94
T017	-53.26

[a] nomenclature given to glycans referring to Supplementary Figures X1 and X2.

[b] glycans also present in tumor cells but in different proportions.

Figure 1.

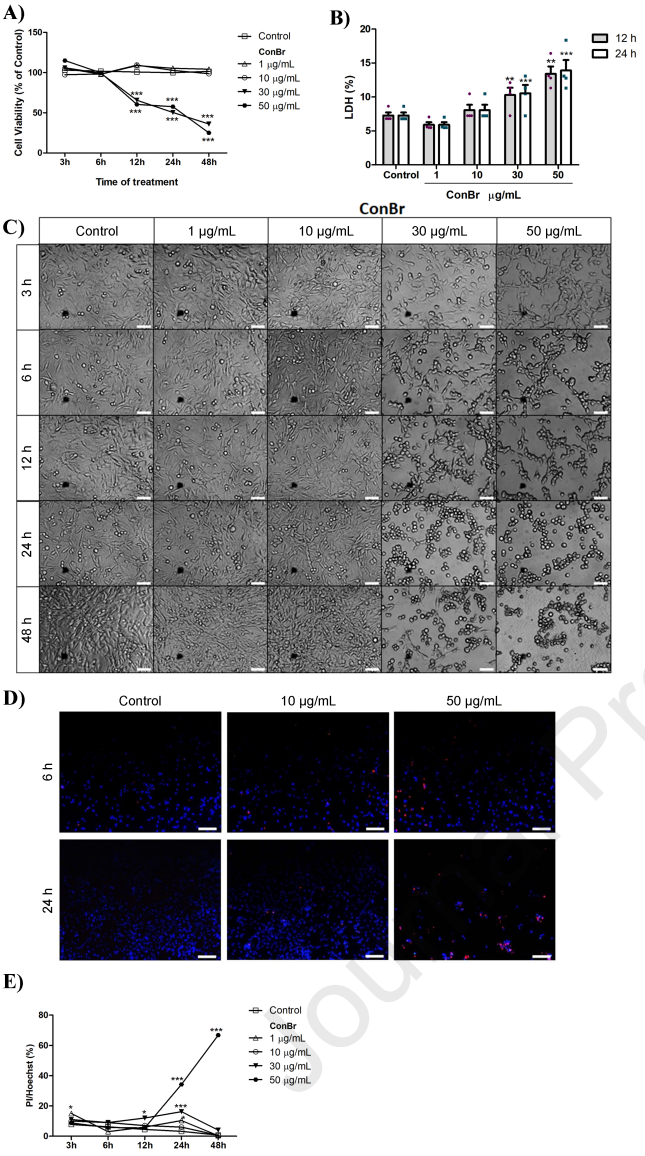

Figure 2.

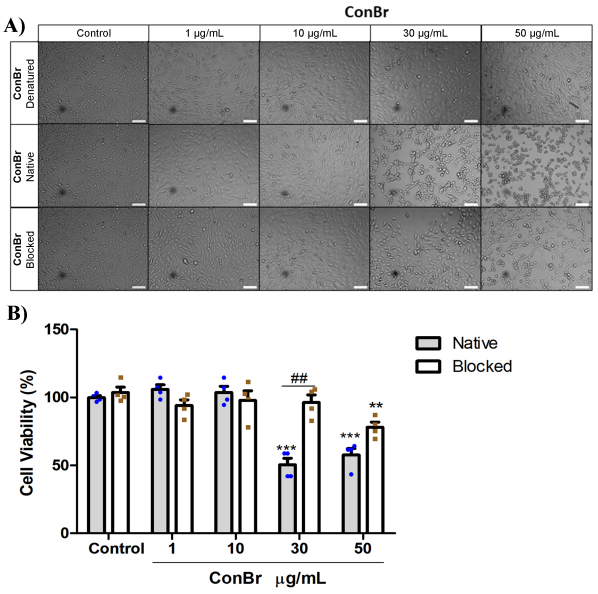

Figure 3.

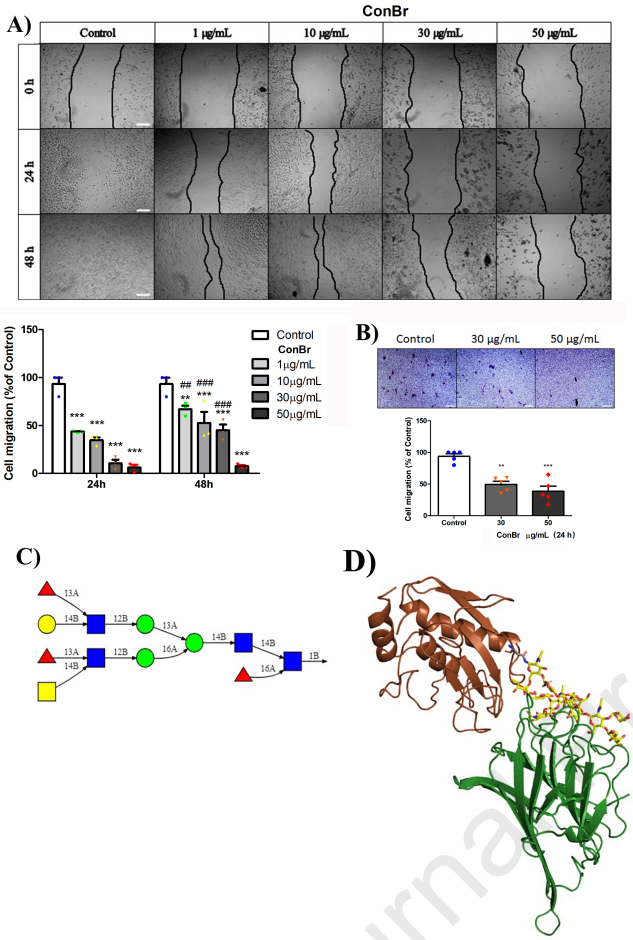

Figure 4.

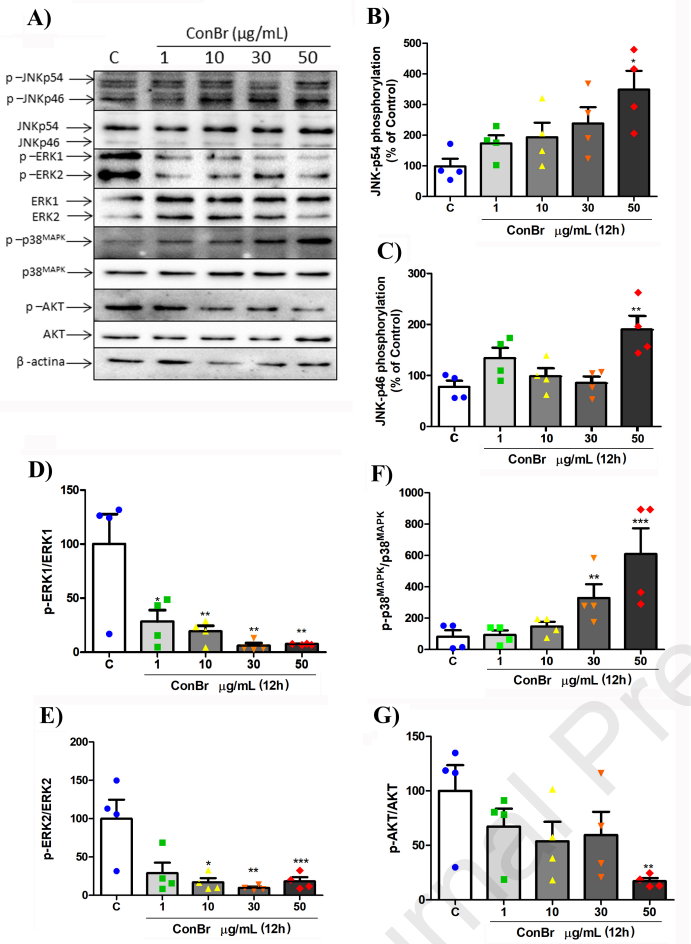

Figure 5.

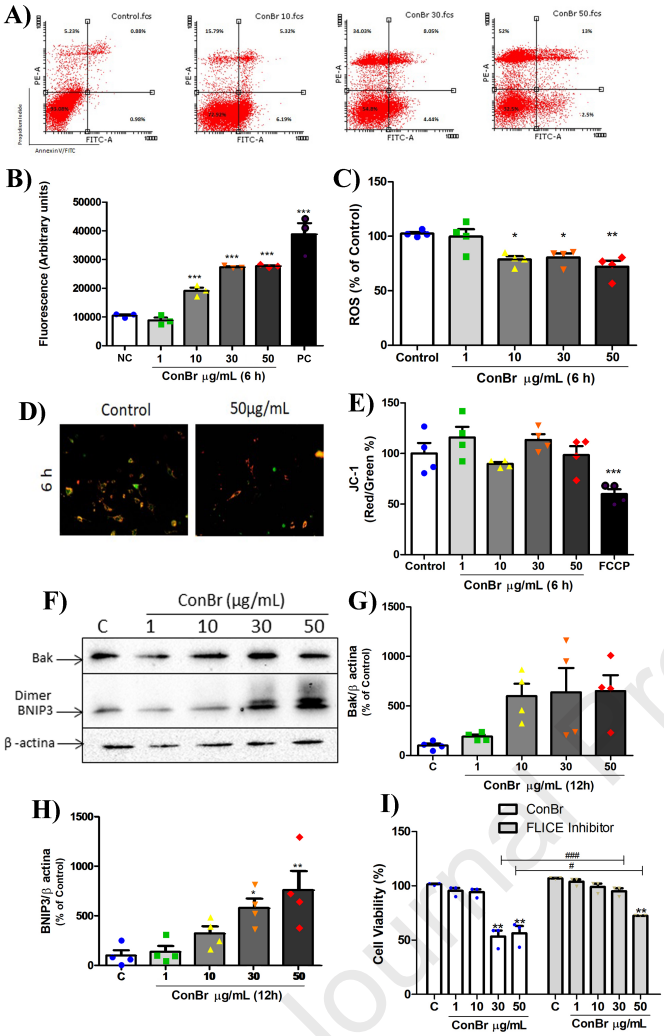

Figure 6.

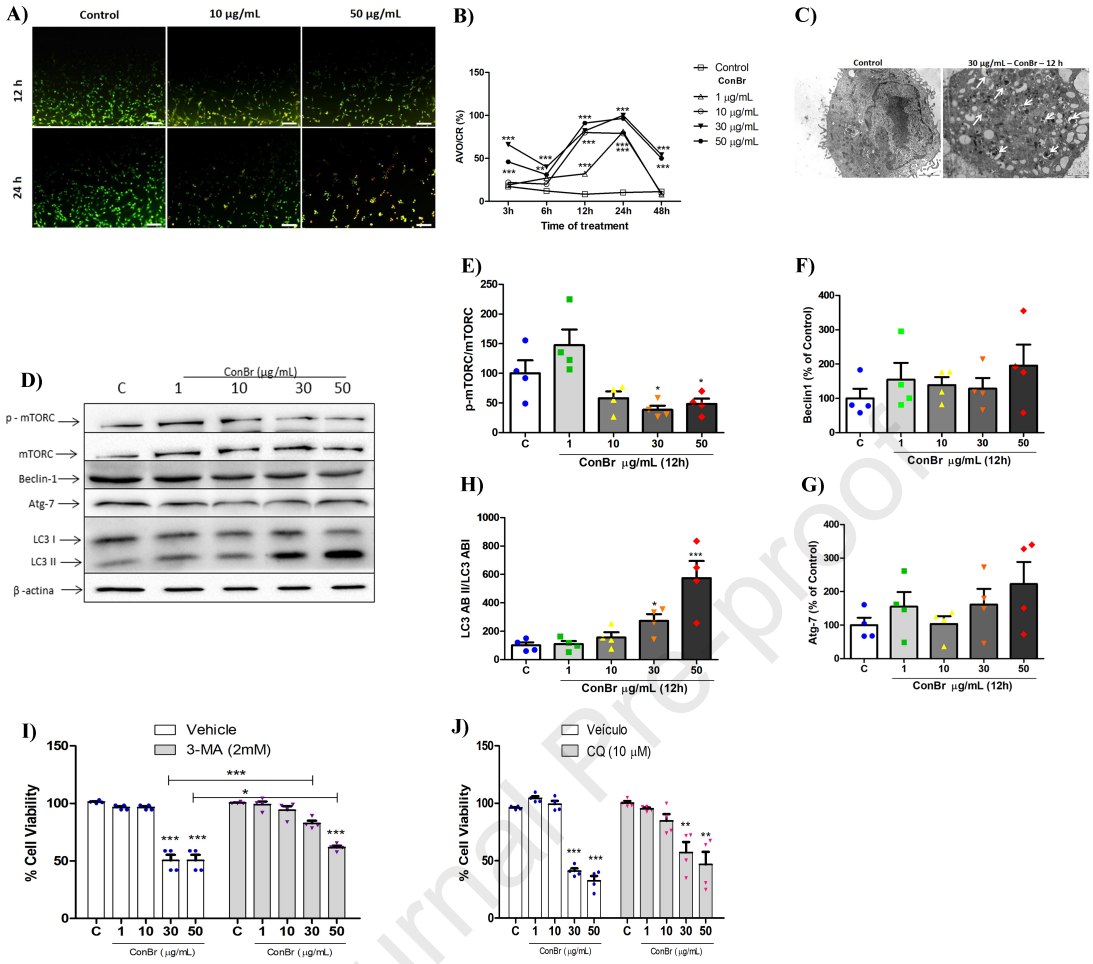

Figure 7.

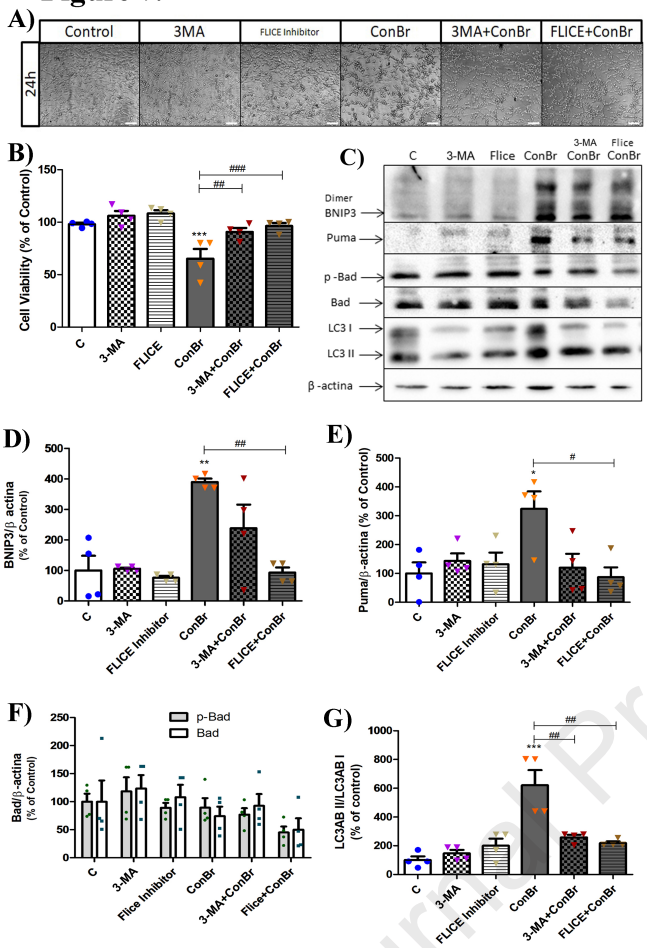

Figure 8.

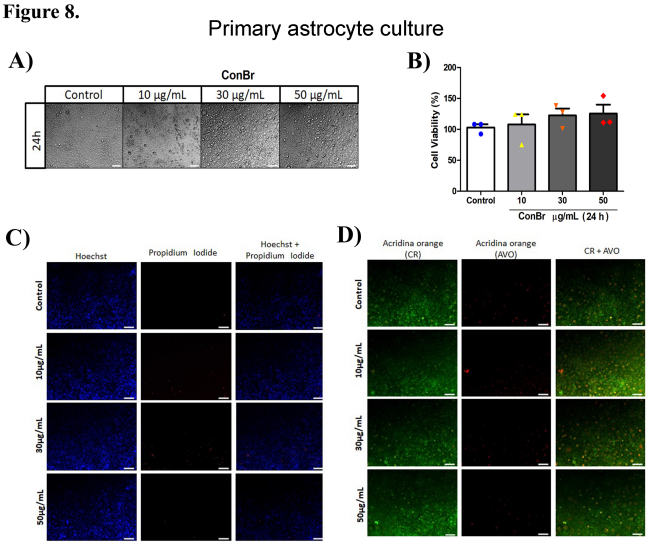

Figure 9.

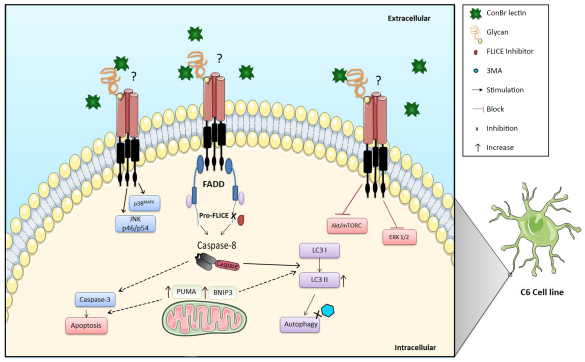

Highlights

ConBr lectin inhibits cell migration and promotes C6 glioma cell death by autophagy.

ConBr-induced cell death and autophagy depends upon caspase-8 activity.

ConBr stimulates $p38^{MAPK}$ and JNK and inhibits ERK, Akt and mTORC1 in glioma cells.

ConBr displays selective cytotoxicity against glioma cells as compared to astrocytes.

UNIVERSIDADE FEDERAL DE SANTA CATARINA
CENTRO DE CIÊNCIAS BIOLÓGICAS
DEPARTAMENTO DE BIOQUÍMICA
Campus Universitário, Florianópolis, SC - Brasil, 88040-900
e-mail: rbleal@gmail.com ; r.b.leal@ufsc.br Tel.:+55 48 3721-5045 Fax: +55 48 3721-9672

October 20th, 2020

Dear Editor,

The authors have declared that there are no conflicts of interest associated with this publication and there has been no financial support for this work that could have influenced its outcome.

Sincerely yours,

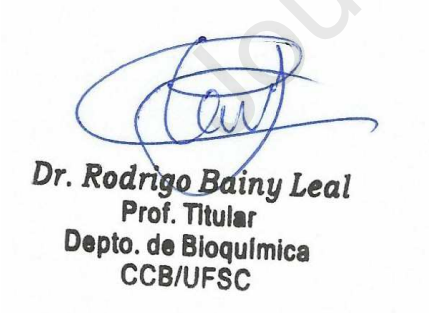

Professor Rodrigo Bainy Leal
Department of Biochemistry
Federal University of Santa Catarina (UFSC)